Aus dem Max-Delbrück Centrum für Molekulare Medizin Berlin

DISSERTATION

Apelinergic system in the kidney: implications for diabetic kidney disease

zur Erlangung des akademischen Grades
Doctor medicinae (Dr. med.)

vorgelegt der Medizinischen Fakultät
Charité – Universitätsmedizin Berlin

von

Tilman Müller

aus Berlin

Datum der Promotion: 18.09.2020

Preface

Parts of this thesis were published in:

Tilman Müller, Anastasia Z. Kalea, Alonso Marquez, Ivy Hsieh, Syed Haque, Minghao Ye, Jan Wysocki, Michael Bader, Daniel Batlle

Apelinergic system in the kidney: implications for diabetic kidney disease, Physiological Reports, 12/2018, 6(23), e13939, doi: 10.14814/phy2.13939

Directory

LIST OF FIGURES

SUMMARY

The bioactive peptides of the apelinergic system and its receptor APJ have been shown to play a protective role in experimental cardiovascular and diabetic kidney disease (DKD). Mechanisms of this renoprotective effect remain to be elucidated. In this study, we examined the localization of APJ within the normal kidney and its kidney expression in the *db/db* model of DKD. The effect of hyperglycaemia and angiotensin II on APJ was examined in cultured podocytes.

In the glomerulus, APJ colocalized with podocyte but not endothelial cell markers. In podocytes stimulated with *Pyr*[1]Apelin-13 a change in the phosphorylation status of the signaling proteins, AKT, ERK and p70S6K was observed, with an increase 15 minutes after stimulation. *Pyr*[1]Apelin-13 decreased activity of Caspase-3 in podocytes after high glucose treatment. Similarly, NADPH-oxidase activity in the hyperglycaemic environment was ameliorated by *Pyr*[1]Apelin-13, reflecting both an anti-apoptotic and anti-oxidative effect of APJ stimulation. In podocytes, APJ mRNA was downregulated in high glucose when compared to normal glucose conditions, and exposure to angiotensin II led to a further significant decrease in APJ mRNA. APJ and preproapelin mRNA levels in kidneys from *db/db* mice were markedly decreased, along with decreased tubular APJ protein by western blotting and immunostaining when compared to *db/m* controls. In conclusion, the apelinergic system is decreased in kidneys from *db/db* mice. Within the glomerulus APJ is mainly localized in podocytes, and in this cell type its activation by *Pyr*[1]Apelin-13 abolishes the pro-apoptotic and pro-oxidative effect of high glucose, suggesting a potential therapeutic role of apelin and emerging agonists with extended half-life for the therapy of DKD.

ZUSAMMENFASSUNG

Für die bioaktiven Peptide des apelinergen Systems und ihres Rezeptors APJ wurden in experimentellen kardiovaskulären Erkrankungen und der diabetischen Nierenkrankheit (DKD) eine protektive Rolle aufgezeigt. Die Mechanismen dieses renoprotektiven Effektes konnten jedoch noch nicht aufgeklärt werden. In dieser Studie untersuchten wir die Lokalisation von APJ in normalem Nierengewebe und seine Expression in dem *db/db* Modell der DKD. Weiterhin wurde der Effekt von Hyperglykämie und Angiotensin II auf APJ in kultivierten Podozyten analysiert.

Im Glomerulus wurde Ko-lokalisation von APJ mit Markern für Podozyten gefunden, allerdings nicht mit Markern für endotheliale Zellen. Stimulation mit *Pyr*[1]Apelin-13 führte in Podozyten nach 15 Minuten zu Veränderungen im Phosphorylierungsstatus der Signalproteine AKT, ERK und p70S6K. *Pyr*[1]Apelin-13 senkte die Aktivität von Caspase-3 und NADPH-Oxidase in Podozyten gezüchtet in hochglukosigem Nährmedium, was den anti-apoptotischen und anti-oxidativen Effekt von APJ Stimulation widerspiegelt. In Podozyten im hochglukosigen Medium wurde eine Herunterregulierung der APJ mRNA im Vergleich zu normoglykämen Bedingungen gefunden und Applikation von Angiotensin II führte zu einer noch weiteren Senkung. Im Vergleich zu den *db/m* Kontrollen waren APJ und Präproapelin mRNA in Nieren von *db/db* Mäusen deutlich gesenkt einhergehend mit reduzierten tubulären APJ Protein Leveln nachgewiesen mittels Western Blot und Immunfärbung. Zusammengefasst zeigt sich das apelinerge System herunterreguliert in Nieren von *db/db* Mäusen. Innerhalb des Glomerulus ist APJ vor allem in den Podozyten lokalisiert und hebt hier nach Stimulation mit *Pyr*[1]Apelin-13 den pro-apoptotischen und pro-oxidativen Effekt von Hyperglykämie auf. Dies könnte auf eine potentielle therapeutische Nutzung von Apelin und Agonisten mit verlängerter Halbwertszeit für die Therapie von DKD hindeuten.

INTRODUCTION

Physiology of the mammalian apelinergic system

APJ is a class A G-protein coupled receptor, consisting of seven transmembrane domains, that shares a 31% identical amino acid sequence with angiotensin AT1 receptor, but does not bind angiotensin II (Ang II) (17). Due to the strong resemblance in sequences APJ is also called angiotensin receptor-like 1 (3). The receptor remained orphaned until the discovery of Apelin in 1998 (3). Apelin is the endogenous ligand for the APJ receptor and was first extracted from bovine stomach (49). Ligand recognition and selectivity is achieved by the receptor's relatively small extracellular domain, especially by the extracellular N-terminal tail's glutamic acid at the 20^{th} position and aspartic acid at the 23^{rd} forming an anionic patch (3, 55). The Apelin gene encodes an initially translated 77-aa pre-proprotein, which is cleaved by proteases to shorter forms, such as Apelin-36 (Apelin 42-77), -17 (Apelin 61-77), or -13 (Apelin 65-77). The pyroglutamate form of Apelin-13 (*Pyr*^{1}Apelin-13), which is more resistant to degradation, is formed through post-translational modification of the N-terminal glutamate (3, 43, 46, 55). The mentioned Apelin isoforms are all biologically active and show different affinities to the APJ receptor (8, 9, 43). Apelin-13 and Apelin-36 are the most abundant and most biologically potent forms (55). All isoforms are characterized by a cationic charge, thus enabling a binding to the anionic patch of the APJ receptor (55). Specifically, the Arginine–Proline–Arginine–Leucine motif and the Lysine–Glycine–Proline–Methionine motif of the Apelin substrates were shown to be important for binding activity and receptor internalization (3). The biological importance of Apelin as a peptide is suggested by its wide tissue distribution and the strict conservation of the last 13aa at the C-terminus (65-77aa) among all species studied (12, 32, 61). APJ signalling is not limited to one subgroup of G-proteins, but rather activates different types depending on the respective cell type. In human umbilical vein endothelial cells, Apelin binding to APJ led to activation of $G_{\alpha 13}$, whereas activation of G_i and $G_{q/11}$ signalling by APJ was found in adipocytes (3). APJ was also described to form heterodimers with other GPCRs such as angiotensin receptor AT1, kappa opioid receptor, neurotensin receptor 1, and bradykinin receptor 1, which possibly modifies properties of each of the respective receptors (3). Since different organs also vary in their expression of proteases, subsequently the processing of Apelin varies, leading to organ-specific changes of the apelinergic system (55). For instance, a direct maturation of proapelin to Apelin-13 was described by proprotein convertase subtilisin/kexin type 3, an enzyme found specifically in heart tissue (3). Consequently, it

was shown that Apelin-13 is the predominant isoform in the heart and also brain, and together with Apelin-17 in plasma, while Apelin-36 is predominantly expressed in the lungs, testis and uterus (3, 55). In summary, the effect of Apelin binding to APJ may differ depending on the organ and the Apelin isoform studied, which may explain the many cellular effects attributed to the apelinergic system. In general, the biological activity of Apelin peptides inversely correlates with peptide length, while the pyroglutamate form of Apelin-13 (*Pyr*[1]Apelin-13) used in several *in vitro* and *in vivo* studies has higher resistance to degradation (3). The 12aa at the C-terminal compose the shortest active Apelin sequence, since Apelin-11 and shorter peptides are inactive (3). Modifications of the terminal residues in Apelin peptides showed that the last carboxyl-terminal phenylalanine plays a critical role in the peptide structure and is important for Apelin to maintain its blood pressure-lowering effects and induce receptor internalization (34). This C-terminal phenylalanine (Phe) amino acid residue of Apelin-13 is cleaved by angiotensin-converting-enzyme 2 (ACE2) (65). So far, no other enzymes have been described to cleave the carboxyterminal Phe from Apelin-13. Hydrolysis of Phe has been assumed to inactivate apelin peptides, which is backed up by findings of absent cardiovascular effects of phenylalanine-cleaved Apelin compared to the original peptide (66). Other studies however have shown that phenylalanine-cleaved *Pyr*[1]Apelin-13 still has affinity to APJ and activates similar pathways to *Pyr*[1]Apelin-13, though being 2- to 5-fold less active (75). In another report, Lee, Saldivia, Nguyen, Cheng, George and O'Dowd (34) exchanged the terminal phenylalanine with alanine, thus forming apelin F13A. In an *in vivo* approach, apelin F13A was found to antagonize the apelin-induced decrease in blood pressure and splanchnic neovascularization (34). However, apelin F13A was also found to act as an apelin agonist in other *in vitro* studies such as intracellular calcium mobilization, adenylyl cyclase inhibition and induction of receptor internalization, rendering it a partial agonist of APJ (3, 43). In conclusion, cleavage or modification of the C-terminal Phe from apelin peptides can be considered to significantly lower or even annihilate effects of Apelin 13.

Localization and effects of the apelinergic system

Messenger RNA (mRNA) encoding preproapelin and APJ receptor have been reported to be expressed in human tissues such as the brain (hypothalamus), placenta, stomach, GI, heart, kidney, adipose tissue, lung and in human endothelial cells (15, 16, 28, 29, 43). The rat homologue of APJ, B78/apj, was detected in the lungs, heart, skeletal muscle, kidney, brain, liver, ovary, and anterior pituitary (46). As stated before, different G-proteins are activated depending on the cell type, and thus

different signalling pathways are effective. However, several main pathways have been described for endothelial cells, smooth muscle cells, neurons, adipocytes, myocytes and even tumor cells including the activation of ERK, p70S6 kinase and AKT (3). Through phosphorylation of key proteins and transcription factors, the effect promoted by these kinases was described to promote cell proliferation, cell survival, migration, and growth as well as metabolic functions including brown adipocyte differentiation (3, 16) (Fig. 1). It has previously been reported that the apelin–APJ system is involved in the regulation of cardiovascular, gastrointestinal and immune functions, as well as having roles in bone physiology, angiogenesis and embryonal development of the cardiovascular system (45). Apelin expression in the hypothalamus has been discussed as regulating fluid homeostasis, food intake and glucose metabolism, while stimulation or inhibition of APJ in the central nervous system may influence behaviour, memory and metabolism (3, 16). In the cardiovascular system, both Apelin and APJ were shown to be present in cardiac myocytes and vascular smooth muscle cells and Apelin is considered to be a strong positive inotrope (14, 28). Furthermore, activation of the apelinergic system leads to peripheral and coronary vasodilatation and enlarged blood vessel diameter in angiogenesis (16). The therapeutic potential of apelins in cardiovascular disease, arteriosclerosis and preeclampsia is a topic of great interest (26, 40, 55, 73, 74, 82). Previous reports have shown that activation of the APJ-Apelin axis exerted a blood pressure lowering effect, increased cardiac output and reduced cardiac fibrosis in mice infused with Ang II, while also being significantly upregulated in patients with heart failure due to failing of the myocardium (8). The effects on blood pressure seem to be endothelium- and nitric oxide synthase-dependent (8). In other studies, Apelin exerted further protective effects. In patients with myocardial infarction and heart failure, treatment with Apelin reduced infarct sizes and improved cardiac parameters such as cardiac output and contractility while decreasing inflammation and increasing cell viability (55). Mitochondrial biogenesis was also found to be increased in cardiomyocytes (3). Through upregulating the expression of antioxidant enzymes such as Catalase in cardiomyocytes, treatment with apelin was found to counter cardiac hypertrophy induced by reactive oxygen species (ROS) (16). In patients with chronic hypertension, stretch mediated cardiac hypertrophy was prevented by Apelin, being likely due to altered ß-arrestin-mediated signalling (52). Conversely, previous publications have shown an association of dysregulated APJ signalling with cardiac hypertrophy, type 2 diabetes mellitus and obesity (3). Also of interest is a recent report showing apelinergic deficiency to promote aging, and conversely, aging is later characterized by a state of multi-organ apelinergic deficiency (50).

In the rat kidney APJ mRNA expression has been reported (15, 46). APJ is highly expressed in the inner stripe (IS), intermediate in the outer stripe (OS) and in the inner medulla (IM), and lowest in the cortex (20). O'Carroll *et al.* (46) found that labelling in the kidney cortex corresponded to an APJ mRNA expression in 40% of the glomeruli, and suggested a role for this receptor in the regulation of blood flow. Studies focusing on the vasculature showed that the apelinergic system regulates Ang II - AT1 receptor signalling (58). It is possible that at the kidney level Apelin may also play a counter-regulatory role in the actions of Ang II. In kidneys, studies on the role of Apelin and APJ in renal hemodynamics showed that Apelin increases medullary blood flow by inducing a vasodilatory effect in agreement with the opposing actions against Ang II regarding blood pressure (21) and vascular tone (11, 83). In a renal disease state, the components of the apelinergic system experience various changes regarding their expression (8, 16, 45). Parts of the apelinergic system may be upregulated in a renal disease state, similar to the apelin upregulation found in patients with cardiovascular disease described above. Both apelin and APJ expression are increased in a mouse model with unilateral ureteral obstruction-induced renal fibrosis, and apelin expression was found to be increased in rats with Adriamycin-induced nephropathy, specifically along the glomerular basement membrane (45). However, renal APJ was found to be downregulated in diabetic mice (8). Of interest are also recent studies examining the role of the apelinergic system in renal pathology. In chronic kidney disease, patients with high Apelin levels were reported to have higher eGFR, lower inflammation markers (e.g. Interleukin-6) and higher adiponectin levels (79). Apelin has been shown to be protective against acute renal injury (5) and diabetic kidney disease (DKD), a dreaded renal complication of a prolonged hyperglycemic state in Diabetes Mellitus (8, 16).

Apelinergic system in Diabetes Mellitus and its complications

Diabetes Mellitus is a metabolic disease characterized by insulin secretion dysfunction and insulin resistance of peripheral insulin receptors (1). The effects are seen in a chronic increase of blood sugar levels leading to damaging and dysfunction of various tissues (1). Current antidiabetic therapy focusses on hypoglycaemic drugs and substitution of insulin (1, 16). In particular, the presence of APJ in pancreatic islet cells led to the hypothesis of an important role of the apelinergic system in insulin and glucose metabolism, since they are considered as key regulators of glucose metabolism and accelerate Diabetes Mellitus Type II development when dysfunctional (3, 16). APJ is expressed in alpha as well as beta cells, but is also found in acinar cells and the pancreatic duct (16). In beta

cells of mice with Type 2 Diabetes parts of the apelinergic system were found to be upregulated. (16). Indeed, Apelin also exerts beneficial effects on blood sugar levels by promoting insulin- and non-insulin dependent glucose uptake, gluconeogenesis, glycogenolysis, fatty acid oxidation, pancreas insulin production, improving insulin sensitivity and reducing body adiposity (3, 16, 43, 55, 74). Furthermore, diabetes-induced reduction of pancreatic islet cell mass and insulin content is improved, while APJ deletion in islet cells leads to reduced beta cell density and beta cell mass, and thus impaired glucose tolerance (3, 55). In adipocytes, the effect of Apelin was seen in the reduction of white adipogenesis while brown adipogenesis as well as browning of white adipocytes was enhanced (3, 16, 55, 79) (Fig. 1). Brown adipose tissue has been shown to improve energy metabolism and increase insulin sensitivity (16). Apelin was also found to reduce free fatty acid release, which is frequently observed to be increased in obesity and a diabetic state, and thus contributes to the development of insulin resistance. Conversely, Apelin deficiency is linked to increased abdominal adiposity and increased free fatty acid levels (16). On the molecular level, the effect of the apelinergic system is seen in changes of glucose regulating proteins, such as increased levels of adiponectin, glucagon-synthase-kinase and glucose transporter 4, while decreasing proteins and transcription factors formerly increased in the diabetic state (55). In skeletal and heart muscle cells, mitochondrial oxidative capacity and mitochondrial biogenesis was found to be improved by Apelin (55). Alterations of the muscle's ultra-structure typically seen in Type II Diabetes Mellitus were prevented and insulin-dependent glucose uptake in muscles was enhanced (3, 16). Improvement of muscular mitochondrial biogenesis was associated with improved insulin sensitivity (16). These mechanisms resulted in a decrease of fat mass, hyperinsulinemia and hyperglycaemia in the diabetic state (3, 16, 55). Conversely, Apelin-KO mice fed with a high fat and carbohydrate diet showed increased insulin resistance, increased visceral body fat, and increased plasma triglyceride levels (3). It should be noted that apelin levels in the hypothalamus are also considered to affect glucose homeostasis and food intake in diabetes (16).

Although different approaches for treating Diabetes exist and are often used successfully, the disease still maintains a high disability and mortality rate through its vascular complications, and innovations are needed to improve long term health outcomes (1, 16). Diabetic cardiomyopathy is a dreaded complication of the cardiovascular system in patients with Diabetes Mellitus, and one of the leading causes of death in diabetic patients (1). A key part in its pathogenesis is played by diabetes-associated microvascular dysfunction (16). Apelin treatment in patients with diabetic cardiomyopathy was found to improve myocardial neovascularization, myocardial vascular density and cardiac repair (37).

Furthermore, increased ROS formation and endothelial cell apoptosis was attenuated (37). These effects were found to be dependent on SIRT3, a mitochondrial enzyme in cardiomyocytes known to ameliorate cardiac hypertrophy, fibrosis and metabolism (78). Apelin treatment also resulted in an increase in VEGF/VEGFR2 and Ang/Tie-2 expression, accompanied by enhanced mobilization and overexpression of bone marrow-derived endothelial progenitor cells to improve neovascularization of ischemic heart tissue (16, 37).

DKD, or diabetic nephropathy, is the leading cause of end-stage renal disease (ESRD) and affects approximately 30% of patients with Diabetes type I and 40% of patients with Type II (1). While advances in antidiabetic therapy have significantly improved general outcome and certain diabetic complications such as diabetic cardiovascular disease, these improvements are not reflected in the occurrence of DKD and ESRD (1). Prevalence of Diabetes and associated DKD are constantly rising around the world due to the global rise in obesity (1, 79). In the years from 1990 to 2012, a worldwide increase of 94% in deaths attributed to DKD was registered (1). Several risk factors contribute to the pathogenesis and progression of DKD, such as family history and race, yet the two most prominent risk factors remain hypertension and hyperglycaemia (Table 1)(1). Regarding the pathogenesis of DKD, it is theorized that metabolic changes in Diabetes Mellitus trigger a chronic tubulointerstitial inflammation, eventually leading to renal injury and fibrosis (16). These critical metabolic changes include hyperaminoacidemia and hyperglycaemia (1, 16). Previous studies have shown that Diabetes Mellitus and hyperglycaemia increase histone acetylation which is associated with an increase in inflammatory markers and chemokines (4, 16). Clinical signs of DKD are reported to be the development of hyperfiltration with progressive albuminuria, decreasing glomerular filtration rate (GFR) resulting in end-stage-renal disease (ESRD) while histologically kidney hypertrophy, thickening of the glomerular basement membrane, podocyte loss, endothelial fenestration and mesangial matrix expansion is found (1, 8, 79). The earliest histological sign is considered to be thickening of the glomerular basement membrane, which is already found after 1.5 to 2 years (1). In a progressed disease state segmental mesangiolysis can be found in kidney tissue, which is associated with the formation of microaneurysms and Kimmelstiel-Wilson nodules (1). Although DKD is a clinical diagnosis, histological changes may still be present even if no clinical signs can be found in the patient (3). It is estimated that 20% of patients with DKD-like kidney lesions do not develop albuminuria or a reduction of eGFR (1). Typically, the changes in kidney tissue are characteristic for both Diabetes Mellitus Type I and II, though lesions are more heterogeneous and

less predictable in Type II (1). Later stages of chronic kidney damage due to DKD include the development of anaemia attributed to a decline in erythropoietin (EPO) formation and disorders in bone and mineral metabolism on the basis of secondary hyperparathyroidism. These complications develop earlier in DKD than in other forms of CKD (1). EPO is produced by peritubular interstitial cells, which are prone to be affected by the tubulointerstitial inflammation caused by Diabetes (1, 16). Furthermore, parathyroid hormone release may also be affected by Diabetes and DKD since levels of parathyroid hormone are lower in DKD compared to other forms of CKD (1). It is now believed that parathyroid hormone secretion is altered by insulin deficiency and/or resistance and patients with DKD are therefore prone to bone metabolism disorders (1). Current therapeutic approaches for DKD include renin-angiotensin-aldosterone (RAS) inhibition with angiotensin-converting-enzyme (ACE) inhibitor or angiotensin-receptor 1 (AT-1) blocker, and dietary sodium restriction and diuretic therapy, but new pharmaceutical targets are needed (1, 3, 16). Interestingly, once DKD has developed, intense glucose control has not been shown to prevent DKD progression or reduce the risk of other cardio- and microvascular complications (1).

In recent studies, properties of the apelinergic system were found to ameliorate key mechanisms in the pathogenesis of DKD. Day, Cavaglieri and Feliers (8) showed that Apelin-13 reduces glomerular hypertrophy and inflammatory markers in the OVE26 model of type 1 diabetes. This is backed up by other studies where apelin treatment in the Akita diabetic mouse model reversed the increase of inflammatory markers such as VCAM1, MCP1 and NF-KB, as well as reducing monocyte infiltration (4). Histone acetylation was inhibited both in the Akita mouse model and in cultured mesangial cells. Conversely, levels of the histone deacetylase 1 enzyme were elevated (4). Thus, an inhibition of diabetes-induced renal inflammation was demonstrated for the apelinergic system (4, 16). Furthermore, apelin treatment restored expression of antioxidant enzymes such as Catalase (8). Upregulation of antioxidant enzymes could be a key outcome of the activation of the APJ-Apelin axis and is discussed as being an important mechanism for its renoprotective effect, as pro-and anti-oxidative pathways have been established as key players in the development of diabetic nephropathy (8, 16, 45). Thus, in their study Day, Cavaglieri and Feliers (8) conclude that the apelinergic system may have protective effects on the development of DKD. Though APJ expression was found to be reduced in kidneys of diabetic mice, treatment with apelin was able to restore contents back to normal levels (8).

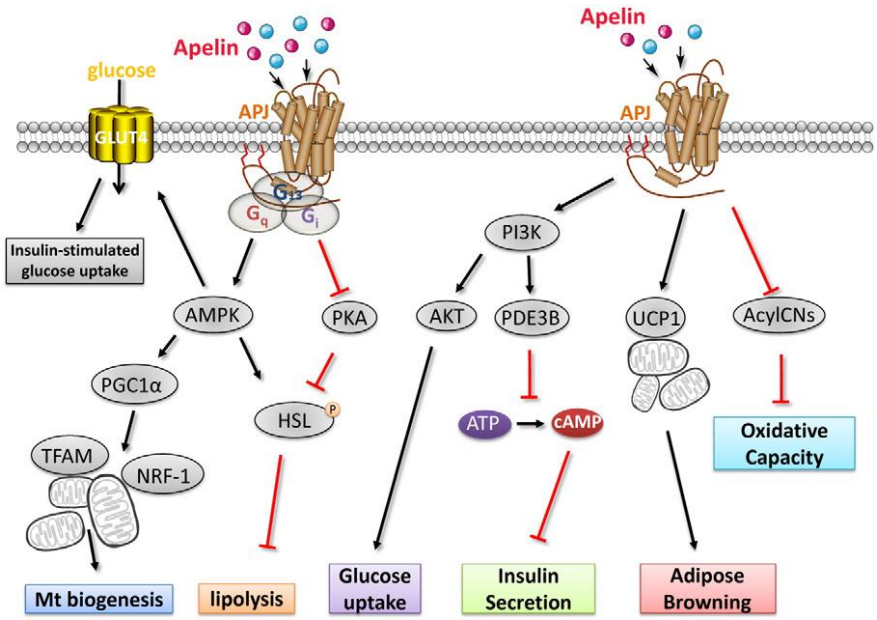

Figure 1. Schematic overview of signal pathways activated by the apelinergic system

Through binding to different G-proteins various effects can be achieved by Apelin stimulation depending on the tissue. In adipose tissue lipolysis is inhibited through HSL phosphorylation or inhibited HSL dephosphorylation. In muscle cells mitochondria biogenesis is improved by AMPK dependent activation of PGC1α, while glucose uptake is enhanced by AMPk (insulin dependent) and AKT (insulin independent). Insulin secretion in the pancreas is inhibited through reduced cAMP levels. Image taken from Hu, He, Li and Chen (16).

Table 1: Risk factors for diabetic kidney disease. Taken from Alicic, Rooney and Tuttle (1).

Risk Factor	Susceptibility	Initiation	Progression
Demographic			
Older age	+		
Sex (men)	+		
Race/ethnicity (black, American Indian, Hispanic, Asian/Pacific Islanders)	+		+
Hereditary			
Family history of DKD	+		
Genetic kidney disease		+	
Systemic conditions			
Hyperglycemia	+	+	+
Obesity	+	+	+
Hypertension	+		+
Kidney injuries			
AKI		+	+
Toxins		+	+
Smoking	+		+
Dietary factors	+		+
High protein intake	+		+

Apelinergic system in embryogenesis

Recently, studies have shown significant developmental defects especially prominent in the cardiovascular system of APJ-KO mice, which were not found in Apelin-KO mice (3). Furthermore, APJ was already found to be expressed in early stages of embryogenesis, whereas Apelin was not found before the end of gastrulation (3). These observations led to the conclusion, and subsequent identification, of the peptide Elabela/Toddler (ELA) as a second ligand of the APJ receptor in human stem cells (16). The ELA-Gene encodes for a 54-amino acid preprotein, which is then cleaved of its 22-amino acid long signal peptide and forms ELA-32, the longest ELA isoform (55). Like Apelin, ELA has multiple bioactive isoforms, which are characterized by a highly conserved sequence of 7 amino acids at the C-terminus with ELA-11 being the shortest active peptide (55). At the time of this study, the ligand ELA has been described exclusively in the adult kidney, prostate, heart and in human pluripotent stem cells (55, 79). Since pluripotent stem cells do not express the APJ receptor, ELA is assumed to bind to a second receptor in this early stage of development (55). ELA was reported to play a crucial role in the migration of mesoendodermal cells during embryogenesis as well as cardiovascular development and inhibited cell apoptosis (55, 79). Its function in the adult organism remains uncertain. In an Apelin knock-out mouse model, supplementation of ELA was found to exert similar effects to Apelin such as blood pressure regulation, fluid homeostasis, cardiac contractility and angiogenesis, suggesting the activation of pathways similar to activation with Apelin (55). In cultured renal cells ELA exerted an anti-inflammatory, anti-apoptotic and anti-fibrotic effect (79). ELA and Apelin isoforms, however, seem to differ in their potency, and occasionally even functionality, while achieving similar physiological effects (67, 76). While therapeutical implications have yet to be studied, ELA could be a potential new predictor of diabetic kidney disease, since serum levels progressively decrease with kidney damage and decreasing eGFR (79).

Perspectives and scientific aim

The pharmacological potential of the apelinergic system is becoming increasingly evident, though some problems remain. The short half-life of current Apelin isoforms complicates its exploration, and the development of isoforms with a larger biodegradation resistance is seen as an important next step (55). Furthermore, very few substrates have been identified to date as agonists or antagonists of APJ, and the exploration of other molecules interacting with the receptor is of special interest, also as potential pharmacologic drugs. To this end, the polypeptide ALX40-4C and ML221 have been

described as the only antagonists of APJ, whereas E339-3D6 is the first, and so far only, non-peptidic agonist (3). To this date, studies of these substrates remain incomplete. For ALX40-4C, a prevention of membrane fusion, calcium mobilisation and APJ internalization was found *in vivo* and *in vitro*, but clinical effects of the antagonism are unknown; ML221 has been shown to inhibit cAMP production and β-arrestin recruitment. E339-3D6 binding to APJ leads to cAMP production and receptor internalization identical to Apelin-13, and an vasorelaxant effect in rat aorta has been shown *ex vivo* (16). Through structural optimization of known ligands and identification of new substrates, it could soon be possible to determine whether the Apelin/APJ axis is an effective target for treatment of diabetes and diabetes associated complications. Similarly, the lately discovered ligand ELA could also be of therapeutical and diagnostical interest, or could even be the first step to a completely new approach of understanding and using the apelinergic system (55, 67). Furthermore, a deeper understanding of the interactions of the Apelin-APJ axis with known pathways and the resulting effects is needed both organ specifically and system wide. Though peripheral administration of Apelin has a positive effect on glucose levels in diabetic mice, studies have shown that central application may have a neutral or even opposite effect on blood glucose levels by stimulating glycogenolysis and gluconeogenesis in the liver (3). Effects of the apelinergic system thus seem to differ in regard to the targeted tissue. It is also of interest that interactions with other systemically active hormone axes such as the Renin-Angiotensin-Aldosterone-System have been described and deserve further examination (3, 8, 16). Through heterodimerization of APJ with the AT1-receptor, a decrease of angiotensin II affinity to its receptor and a modification of intracellular signaling pathways is achieved, which may prove to be a new interesting approach to treating pathological conditions characterized by RAS overactivity (3).

Our study was aimed at determining the localization of the APJ receptor within the kidney glomerulus and examining its regulation by hyperglycaemia and Ang II as well as signalling by Apelin-13 using cultured podocytes. The influence of the apelinergic system on apoptotic and oxidative pathways was investigated using the respective activity assays. Further we examined known renal enzymes and also compared kidney glomerular and tubular cells for their degrading capacity of Apelin-13. Changes of Apelin-13 degrading enzymes were then studied under normo- and hyperglycaemic conditions. Finally, the *db/db* mouse was used to examine the kidney expression of the apelinergic system in a model of type 2 diabetes. The influence of current RAS- inhibiting therapy on the expression levels

was studied using the AT-1 receptor blocker telmisartan. Furthermore, changes of the RAS and apelinergic system were compared between the *db/db* mouse and their lean littermates.

MATERIALS AND METHODS

Animal model and tissue preparation

Obese *db/db* mice (C57BLKS/JLepr) were used as a model of type 2 diabetes and their lean littermates (*db/m*) served as nondiabetic controls (Jackson Laboratory, Bar Harbor, ME). We used young (8 wk of age) female *db/db* mice to study an early phase of diabetes (3-4 wk of onset) and 24-32 week old female *db/db* mice which exhibited kidney lesions consistent with early diabetic nephropathy (36). The Institutional Animal Care and Use Committee approved all procedures. Kidneys and hearts from these mice were removed quickly, cut longitudinally, and half of kidney and heart sections were stored at -80^{o}C for protein and RNA analysis. The remaining half of kidney sections was fixed with 10% buffered formalin phosphate (Fisher Scientific, Hanover Park, IL) overnight. After paraffin embedding, tissue sections (4 µm) were deparaffinized in xylene and rehydrated through graded ethanol series before use.

Kidney histology

For histological evaluation, kidneys were cut longitudinally and fixed with 10% buffered formalin phosphate (Fisher Scientific, Pittsburg, PA, USA). Paraffin sections were stained with hematoxylin and eosin and periodic acid-Schiff. Glomerular hypertrophy was quantified by measuring the glomerular tuft cross-sectional area with a computer image analysis system (Image J, NIH). Glomerular hypertrophy was assessed by measuring the tuft area from glomeruli in which the vascular pole was evident (using 20 glomeruli per section). This was performed to reduce the possibility of including tangentially cut glomeruli (57). Glomerular images were obtained digitally using the Tissue Gnostic Acquisition platform. Total glomerular area was traced, and calculated using Image J (NIH) analysis software. Mesangial matrix expansion and glomerular cellularity was graded by a masked renal pathologist using a semiquantitative score.

Preparation of RNA and protein extracts

Kidney and heart sections were used to extract total RNA using TRIZOL® (Thermo Fisher Scientific, Waltham, MA) following the manufacturer's instructions under a fume hood. After adding 1000 µl of TRIZOL to each sample, the samples were mixed at 4°C for 30 minutes (min). Next, 360 µl of

Chloroform were added and the mixture was incubated at room temperature for 3 min. Samples were centrifuged at 11,400 rotations per minute (rpm) at 4°C for 15 min using a GS-6R centrifuge (Beckman Coulter, Brea, CA) and the upper clear liquid layer was transferred into a fresh vial. 600 µl of Isopropanol were added and the tube was thoroughly mixed. The mixture was incubated at room temperature for another 10 min, before centrifuging it at 14,000 rpm for 10 min. The supernatant was removed and the pellet washed with 500 µl of 75% ethanol in distilled water. After centrifuging the tubes at 14,000 rpm for 10 min, the supernatant was again removed and the pellet dissolved in 100 µl of RNA storage solution (Thermo Fisher Scientific, Waltham, MA), incubated at 56°C for 10 min and stored at -80°C.

Total RNA was quantified and tested for purity by optical density (OD) absorption ratio OD260 nm/OD280 nm with a spectrophotometer (GeneQuant Pro, Biochrom, Cambridge, United Kingdom). RNA was reverse transcribed using Reverse Transcription Kit (Thermo Fisher Scientific, Waltham, MA) following manufacturer's protocols (see below) and cDNA was stored at -20°C for further analysis. For protein extracts, kidney sections were washed with Phosphate Buffered Saline (PBS) over ice, and protein was extracted using mammalian protein extraction buffer (MPER, Pierce) supplemented with a protease inhibitor cocktail (Sigma-Aldrich, Saint Louis, MO) and PMSF, following manufacturer's instructions. Protein concentrations in protein homogenate supernatants were measured with the BCA assay method (see below). Supernatants were stored at -70°C and used for detection of proteins of interest.

Reverse Transcription and RT-qPCR

Constant amounts of 2.5 µg of extracted kidney and heart RNA were reverse transcribed to synthesize complementary DNA (cDNA). Synthesis of cDNA was performed using a Reverse Transcription Kit on a GenAmp PCR System 9700 (both Thermo Fisher Scientific, Waltham, MA). Reverse Transcription Master Mix was prepared by mixing 84 µl of distilled water with 20 µl of MultiScribe Reverse Transcriptase, 40 µl of both Reverse Transcriptase Buffer and Reverse Transcriptase Random Primer solution, plus 16 µl of dinucleoside triphosphate (dNTP) mix. For each sample 10 µl of the Master mix were added to 10 µl of the RNA sample, before thermal cycling was initiated using the suggested cycling parameters (25°C for 10 min, 37°C for 120 min, 85°C for 5 min). The mRNA expression for the genes of interest was quantified by RT-qPCR on a 96-well plate using a TaqMan Gene Expression Master Mix on a Step One Plus PCR System (both Thermo Fisher Scientific,

Waltham, MA). TaqMan PCR Master Mix was prepared by mixing 12.5 µl of the 2x TaqMan PCR Master Mix with 1.25 µl of 20x Primer/Probe Mix for APJ or preproapelin and 11.5 µl of distilled water. 24 µl of the TaqMan PCR Master Mix were then added to 1 µl of cDNA. PCR reactions were carried out using Assays-on-Demand^{TM} Gene Expression Products (Thermo Fisher Scientific, Waltham, MA) following the suggested RT-qPCR protocol for all investigated factors: denaturation for 10 min at 95°C, 40 cycles of a three segmented amplification and quantification program (denaturation for 10 sec at 95°C, annealing for 15 sec at the primer specific temperature (95°C), annealing/extension for 1 min at 60°C). Reactions were performed in duplicates. mRNA expression for preproapelin and APJ was normalized against glyceraldehyde-3-phosphate dehydrogenase (GAPDH) mRNA expression. GAPDH was chosen as internal control, since the levels were consistent among kidney and heart tissues as described in previous reports (43). Primers were ordered from Thermo Fisher (GADPH: Mm99999915_g1; APJ: Mm00442191_s1; Preproapelin: Mm00443562_m1).

Western Blot

Protein expression for APJ was studied using protein extracts from mouse kidney lysates (~20µg), which were separated on 10% Bis-Tris Novex precast gels (Thermo Fisher Scientific, Waltham, MA) with MOPS buffer, after denaturation in reducing sample buffer. Proteins were transferred to treated 0.4µm PVDF membranes (Millipore, Billerica, MA) by sodium dodecyl sulfate (SDS)-electrophoresis in a Criterion electrophoresis chamber system (Biorad, Hercules, CA). For electrophoresis samples were denatured at 95°C for 5 min, and then loaded into the gel along with the molecular weight marker (Thermo Fisher Scientific, Waltham, MA). A running buffer (Thermo Fisher Scientific, Waltham, MA) was poured into the chamber and the electrophoresis started at 75 V for 20 min, and then increased to 120 V for 2h. Transfer buffer was prepared by mixing 150 ml of 10x concentrated transfer buffer with 1,050 ml distilled H_20, 300 ml Methanol and 3 ml SDS 10%. PVDF membranes were prewetted with 100% Methanol. Transfer was performed in the electrophoresis chamber with the transfer buffer at 12 V overnight. TBS-Tween solution was prepared by mixing 10 ml of 10% Tween solution (Sigma-Aldrich, Saint Louis, MO) with 10 ml of 1M Tris-HCl pH 8 and 980 ml of distilled H_20 plus 8.8 g NaCl. PVDF membranes were blocked using 5% nonfat dry milk in 0.1% v/v Tween-30 Tris-buffered saline (TBS-T) for 1h, washed five times with TBS-Tween, and were later immunoblotted using a primary antibody for APJ (goat polyclonal IgG

1:500, raised against a peptide mapping within a C-terminal cytoplasmic domain of APJ (Santa Cruz Biotechnologies, Dallas, TX) for 2h, and its corresponding HRP-linked secondary antibody overnight after washing the membrane another five times. The respective blocking peptide for APJ was used on the same membrane to verify the specificity of the bands detected in kidney samples. For further studies, we focused on the 42 kDa band, based on the reported molecular size of the monomeric APJ (2), and the uncertainty as to the identity of the extra bands which were also erased by the blocking peptide in kidney lysates (Figure 1). A positive control with 293T whole cell lysate from cells transfected with human APJ was also used (Santa Cruz Biotechnologies, Dallas, TX) along with the kidney samples (Fig. 2).

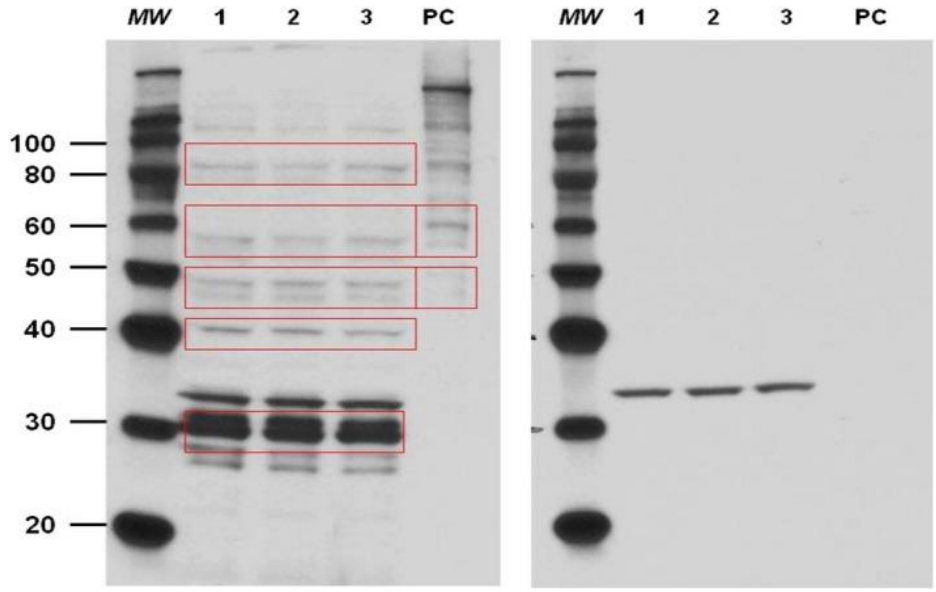

Figure 2. Immunoblot analysis for APJ in mouse kidneys

Immunoblot analysis for APJ in mouse kidneys (n=3) without (left) and with (right) blocking peptide incubation. MW: molecular weight marker; PC: positive control, whole cell lysate from 293T transfected cells with human APJ; 1,2,3: lysates from three different mouse kidneys; red rectangular shapes highlight the main bands erased by the blocking peptide.

In all experiments detection of signal was performed using Amersham ECL Plus reagents, and films were developed and quantified by densitometry using ImageJ Software. In many cases, to confirm equal loading of total protein into each lane, membranes were stripped and probed for the control protein β-tubulin (rabbit polyclonal IgG for β-tubulin, Santa Cruz Biotechnologies, Dallas, TX).

Immunohistochemistry

Kidney sections (4 μm) were deparaffinized and rehydrated. Antigen retrieval was performed with a pressure cooker at 120°C in target retrieval solution (Agilent Technologies, Santa Clara, CA). Endogenous peroxidase activity was blocked with 3% hydrogen peroxide (Thermo Fisher Scientific, Waltham, MA). The primary antibodies for anti-APJ (1:100; rabbit antibody, Neuromics, Edina, MN) and WT-1 (1:400; rabbit antibody, Santa Cruz Biotechnology, Dallas, TX) were applied overnight, and one slide in each set of experiments was incubated with only non-immune serum to be used as negative control. Sections for APJ and WT-1 staining were washed and incubated with goat anti-rabbit IgG conjugated with peroxidase-labeled polymer (Agilent Technologies, Santa Clara, CA). Peroxidase labeling was revealed using a liquid diaminobenzidine substrate-chromagen system (Agilent Technologies, Santa Clara, CA). Sections were counterstained with hematoxylin (Sigma-Aldrich, Saint Louis, MO) and dehydrated, mounted with Permount (Thermo Fisher Scientific, Waltham, MA), and cover-slipped. For anti-APJ staining, sections were examined and photographed with a Nikon Eclipse 50i microscope for semi-quantitative and qualitative observations and comparisons. For assessment of the intensity of APJ kidney staining, a semiquantitative analysis of the immunoperoxidase stained sections was done based on a fooling scale: 0- no staining; 1-weak staining; 2-strong staining. Sections were examined independently by two observers, who assessed staining intensity of each slide of either 5 viewing fields (for tubular staining) or 25 glomeruli (for glomerular tuft staining). A composite score was then generated for each mouse to compare APJ staining in *db/m* and *db/db* mice.

For podocyte count, two blinded observers counted WT-1 stained nuclei in 20 glomeruli from each kidney section.

Confocal Immunofluorescence Microscopy

The paraffin-embedded kidney sections (4 μm) were deparaffinized and rehydrated. After antigen retrieval, sections were permeabilized with 0.5% Triton-X100 in PBS for 5 min and blocked with 5% normal donkey serum in PBS for 1 h at room temperature in a humidified slide chamber. The sections were incubated with primary antibodies diluted in 5% donkey serum in PBS overnight at 4°C. The primary antibodies used for the immunofluorescence were anti-APJ (1:200; rabbit antibody, Neuromics, Edina, MN) and one of the specific cell type markers. For the APJ antibody used for IF, there is no commercially available peptide immunogen. This anti-APJ antibody, however, had been

validated by the producer using APJ-transfected COS-7 cells (Neuromics, Data Sheet). Moreover, in a study by Farkasfalvi *et al.* (10) in addition to the antibody we used, a second APJ antibody directed against a different region of the receptor was used to ensure robust results. They determined that both antibodies showed the same staining pattern and thus both were equally specific. As podocyte markers, we used: anti-nephrin (1:100; Santa Cruz Biotechnologies, Dallas, TX), which localizes specifically in the slit diaphragm (80); an antibody against synaptopodin (1:100; Santa Cruz Biotechnologies, Dallas, TX), which is an actin-associated protein in the podocyte foot process (63); anti-podocin (diluted 1:100; Santa Cruz Biotechnologies, Dallas, TX), which is specific for the basal pole of podocyte along the glomerular basement membrane (51), as well as anti-WT-1 (diluted 1:100; Santa Cruz Biotechnology, Dallas, TX) and DAPI (Santa Cruz Biotechnolgies, Dallas, TX), for specific podocyte nuclear staining. Platelet-endothelial cell adhesion molecule (PECAM-1) antibody (1:100; Santa Cruz Biotechnologies, Dallas, TX) was used as an endothelial cell marker of glomerular endothelial cells and α-smooth muscle actin antibody (diluted 1:200; Sigma-Aldrich, Saint Louis, MO) was used to stain vascular smooth muscle (77). Desmin, a gift from J Meiner, was used as a marker of mesangial cells (38). Antibodies against ACE2 (diluted 1:200, affinity purified (77)), ACE (77) and aquaporin 2 (diluted 1:200, Santa Cruz Biotechnology, Dallas, TX) were used for colocalization studies within proximal and collecting tubules. Sections were washed with PBS-T three times and then incubated for 45 min with one of the respective fluorescent secondary antibodies (diluted 1:200; Alexa Fluor 488 donkey anti-rat, Alexa Fluor 555 donkey anti-rabbit, Alexa Fluor 647 donkey anti-goat, and Alexa Fluor 647 donkey anti-mouse IgG; Molecular Probes, Eugene, OR). Sections were washed three times and cover slips were placed carefully on top of one drop of Prolong Gold antifade reagent (Molecular Probes, Eugene, OR), and sealed with nail polish. Negative controls for immunofluorescence staining were performed by substitution of non-immune serum for the primary antibodies in adjacent sections (30). All slides were visualized with a Zeiss LSM 510 confocal microscope (Carl Zeiss, Jena, Germany).

ELISA measurements in urine and plasma samples

Plasma and urine samples of *db/m* and *db/db* mice were tested for Apelin concentration (pg/ml) using a fluorescent enzyme-linked immunosorbent assay (ELISA) directed against the C-terminus of Apelin-12 (Phoenix Pharmaceuticals, Belmont, CA) following the manufacturer's protocol. The kit

used is designed to detect the C-terminus of other active forms of Apelin, including Apelin-36 and Apelin-13 (sensitivity: 15.8 pg/ml).

In urine samples, we also measured Angiotensinogen (AOG) by a quantitative solid-phase sandwich ELISA (IBL-America, Minneapolis, MN; sensitivity: 30 pg/ml) as well as Ang II using an EIA Kit from Cayman Chemical (Ann Arbor, MN; sensitivity: 1 pg/ml). This assay had less than 0.001% cross-reactivity with Ang (1-7) and 4% cross-reactivity with Ang I(1-10). Creatinine concentration was assessed using the Jaffe method (Creatinine Companion, Exocell, Philadelphia, PA) and used for correction of the urinary values of Apelin-12, AOG and Ang II.

For urinary peptide measurements, an aliquot of 100 µl of freshly collected urine was transferred into tubes kept on ice at 4°C containing a 10X concentrated cocktail of peptidase inhibitors: 25 mM EDTA, 0.44 mM o-phenanthroline, 1 mM chloromercuribenzoic acid (PCMB), and 120 mM pepstatin A in PBS mixed thoroughly. The urine with inhibitors was then stored at -80°C until the extraction. Angiotensin peptides were extracted from urine using reverse-phase phenyl silica columns (Thermo Scientific cat. no. 60108-386, 100 mg) according to the manufacturer's instructions. Columns were prewashed with 1 ml of 100% methanol and the urine samples were applied. After washing the columns with 1 ml of distilled water, 0.9 ml of methanol was used to elute the absorbed peptides. The eluant was transferred to a new tube and evaporated in a GS-6R centrifuge with heating (Beckman Coulter, Brea, CA). The dried extract was diluted in 0.4 ml of ELISA Buffer for the respective assays. Urinary angiotensin II and Apelin levels were measured using EIA kits with 100 µl of the diluted extract for the angiotensin II ELISA (Cayman Chemicals, Ann Arbor, MI), 50 µl for the Apelin-12 ELISA (Phoenix Pharmaceuticals, Mannheim, Germany) and 10 µl for the AOG ELISA (R&D Systems, Minneapolis, MN) according to the manufacturer's protocol.

Cell culture

Conditionally immortalized mouse podocytes generated by Dr. Peter Mundel (Massachusetts General Hospital, Boston, MA) were cultured as described previously (6, 35, 53). For the studies, passages 23-28 were used. The cultured cells exhibited epithelial morphology and were characterized as podocytes by detection of the podocyte-specific markers podocin, synaptopodin and nephrin, by immunofluorescence staining (see Results). The cells were allowed to differentiate for at least 2 weeks at 37°C without γ-interferon in DMEM (Gibco Laboratories) containing 5.5 mM glucose and with 5% heat-inactivated FBS (Gibco Laboratories). The medium was refreshed every 3 days, and the cells

were sub-cultured upon confluence. These cells were then used for apoptosis and cell signaling studies. For qPCR studies, podocytes (Probetex, San Antonio, TX) were starved 24h before measurements at 37°C in a 5% CO_2 atmosphere in 5.5 mM glucose DMEM (low glucose condition, LG), or 25 mM DMEM (high glucose condition, HG) without FBS. In a second approach, podocytes were starved 24h before measurements under a high glucose condition with or without addition of 0.1 µM of Ang II. In this setting media was exchanged once after 12 hours. The medium was aspirated after 24h and the dishes were washed with 4 ml of ice cold PBS followed by RNA extraction by TRIZOL (as described above). For cell culture studies, the PCR was performed using a SYBR Green qPCR Master Mix Kit (Thermo Fischer Scientific, Waltham, MA), by applying the standard cycling parameters mentioned above and using primers (IDT, Coralville, IA) specifically designed for this type of qPCR (see below). Primers were diluted to a concentration of 20 µM/µl. For each sample a total of 2 µl of cDNA was mixed with 12 µl of distilled water, 5 µl of SYBR GREEN Master Mix and 0,5 µl of each forward and reverse primer. The total volume was 20 ul for each well. Again, GADPH was used as an internal control.

Table 2: Primers for RT-qPCR

Primer	Sequence 5'-3'	Accession Number
APJ F	TTT GGA GCA GCC GAG AAA	AB033170.1
APJ R	GTC AAA CTC CCG GTA GGT ATA AG	AB033170.1
Apelin F	TCC AGA TGG GAA AGG GCT	AB023495.1
Apelin R	CTG TCT GCG AAA TTT CCT CCT	AB023495.1
GADPH F	ACT CCC ATT CTT CCA CCT TTG	AB017801.1
GADPH R	CCC TGT TGC TGT AGC CAT ATT	AB017801.1

Cell signaling assays

Activation of cell signaling proteins was evaluated by western blot using phosphorylation-specific antibodies on podocytes stimulated with *Pyr*[1]-Apelin-13. Podocytes were seeded in 100mm cell culture plates (~10^6 cells/plate). Sub-confluent cells were serum-deprived overnight and then stimulated with 100 nM *Pyr*[1]-Apelin-13 (Bachem, Bubendorf BL, Switzerland) for 1, 5, 15 and 60 min. Protein was then extracted using a mammalian protein extraction reagent (MPER, Pierce) supplemented with protease (Sigma-Aldrich, Saint Louis, MO) and phosphatase (Roche, Basel,

Switzerland) inhibitor cocktails. Lysates containing equal quantities of total protein were separated in 10% Bis-Tris Novex precast gels and proteins were transferred to nitrocellulose membranes (Millipore, Billerica, MA). After blocking the membranes with 5% BSA solution, membranes were incubated overnight with primary antibodies for phospho-specific and total AKT, p70S6K and ERK (Cell Signaling), and with their corresponding HRP-linked secondary antibodies. Detection of signal was performed using Amersham ECL Plus reagents, and the films were developed and quantified by densitometry using ImageJ Software and the FLx800 reader (Biotek, Winooski, VT).

Caspase-3 Assay

The assay was performed using a kit (Cayman Chemical, Ann Arbor, MI) containing Caspase-3 assay buffer, lysis buffer and substrate and inhibitor solution. Conditionally immortalized podocytes were serum starved 24 h before the experiment with RPMI 1640 and 0.2% fetal bovine serum and seeded onto a 96-well plate. *Pyr*[1]-Apelin-13 (100 nmol) was diluted in RPMI medium with high glucose (25 mM) or normal glucose (11.1 mM) content, and 100 µl of the solution was put onto the cells. Cells were incubated at 37°C overnight in a 5% CO_2 atmosphere. The plate was centrifuged at 800g for 5 min and the medium was aspirated; 200 µl of Caspase-3 assay buffer was added to each well and the plate was centrifuged again at 800g for 5 min. After adding 100 µl of cell-based assay lysis buffer to each well, the plate was placed on an orbital shaker for 30 min at room temperature. The plate was then centrifuged for 10 min at 800g. The supernatant of each well (90 µl) was then transferred to a corresponding well on a black 96-well plate, and 10 µl of Caspase-3 Assay Buffer or 10 µl of Caspase-3 inhibitor solution was added. Finally, 100 µl of Caspase-3 substrate solution was pipetted in each well and the plate was incubated for 30 min at 37°C. Activity was measured at 485 nm excitation and 535 nm emission using a microplate fluorescence reader FLx800 (Biotek, Winooski, VT).

NADPH-Oxidase Assay

The assay was performed using the NADPH-Oxidase Assay Kit (Cayman Chemical, Ann Arbor, MI) containing NADPH-Assay buffer, NADPH lysis buffer, protease inhibitor cocktail and lucigenin. Conditionally immortalized podocytes were serum starved 24h prior to the experiment with RPMI 1640 and 0.2% fetal bovine serum. Again, *Pyr*[1]-Apelin-13 (100 nmol) was diluted in RPMI medium with high glucose (25 mM) or normal glucose (11.1 mM) content and 100 µl of the solution was put

onto the cells. Cells were incubated at 37°C overnight in a 5% CO_2 atmosphere. The plate was washed twice with cold PBS solution and the cells were transferred to 1.5 ml tubes. The tubes were centrifuged at 1,200 for 10 min and the medium was aspirated; 300 µl of NADPH lysis assay buffer and 3 µl of protease inhibitor cocktail was added to each tube. The protein concentration was measured using the BCA assay and the sample was adjusted to a concentration of 1 µg/µl. A sample volume of 20 µl was then transferred to 80 µl NADPH Assays Buffer solution. Just before measuring, 900 µl of a solution containing 878 µl NADPH Assays Buffer plus 5 µl Lucigenin and 17 µl NADPH was added to each sample. Activity was measured at 485 nm excitation and 535 nm emission using a microplate fluorescence reader FLx800 (Biotek, Winooski, VT).

Effect of AT1-receptor blockade on kidney APJ and preproapelin mRNA levels

Telmisartan, a specific Ang II receptor antagonist, was given to *db/db* mice for 11 weeks starting at the age of 13 weeks. Mice were assigned to drink either tap water (*n*=6) or tap water with telmisartan (Boehringer Ingelheim, Ingelheim am Rhein, Germany) at a dose of 2 $mg*kg^{-1}*day^{-1}$ (*n*=6). For telmisartan administration, mice were weighed and the daily fluid intake per mouse was recorded to estimate the concentration of the compound needed to be added to the drinking water.

Degradation studies using Phenylalanine-Assay

The assay was performed using the Phenylalanine detection kit from Sigma-Aldrich (St. Louis, MO, USA) containing Assay buffer, Enzyme mix and Developer mix. For assessing the total C-terminal Apelin-13 degradation *in vitro*, human and mouse recombinant Angiotensin-Converting-Enzyme 2 (ACE2) and mouse recombinant Prolylendopeptidase (PEP) were ordered (R&D Systems, Minneapolis, MN), and diluted to a concentration of 1 µg/µl. The amount of 10 µl of mrACE2 or mrPEP were then added to a mix of 10 µl Apelin-13 (10^{-3} M), 6 µl distillated H_20, 3 µl TBS solution 10x concentrated and 1 µl zinc chloride ($ZnCl_2$) (10^{-4} M) and incubated at 37°C with gentle agitation in a thermomixer (Eppendorf, Hamburg, Germany). Reactions were stopped after 30 minutes by heat inactivation at 80°C. After adding 68 µl Phenylalanine-Assay Buffer from the kit samples were put on ice for 5 min. Then 1 µl of Enzyme and 1 µl of Developer mix were added to the samples. The total volume was 100 µl. The samples were incubated at 37°C for another 20 minutes protected from

sunlight, transferred to a 96-well plate and measured by microplate fluorescence reader FLx800 (Biotek, Winooski, VT).

For studying Apelin-13 degradation *ex vivo* isolated for kidney glomeruli and tubules, protein concentration of each sample was measured by BCA assay according to instructions by the manufacturer, and samples were diluted accordingly to a concentration of 1 µg/µl for the activity assays. For assessing the total C-terminal Apelin-13 degradation, 10 µl of glomerular or tubular tissue was incubated with 10 µl Apelin-13 (10^{-3} M), 6 µl distillated H_20, 3 µl TBS solution 10x concentrated and 1 µl $ZnCl_2$ (10^{-4} M) for 30 min at 37°C for endpoint fluorescence reading as described above. In a second approach, 1 µl of the specific ACE2-Inhibitor MLN-4760 and/or PEP-Inhibitor ZPP (each 10^{-4} M) were added to determine the influence of the respective proteases on Apelin-13 degradation. Samples for kidney glomeruli and tubules from each mouse were run on the same plate, respectively. Endogenous substances like pyruvate in the tissue samples can interfere with fluorometric assays and lead to incorrect readings. To rule out the influence of these substances, a second set was run for each organ at the same time without Apelin-13 but in total 16 µl of distillated water. Activity is reflected by the difference between the values of the first set and the second set without Apelin-13.

Kidney Glomeruli isolation

Dynabead solution was prepared by adding 200 µl of magnetic beads (Thermo Fischer, Waltham, MA) to 2 ml 0.2M Tris-HCl (pH 8.5) in DNase-Free tube. The mixture was incubated at room temperature overnight. Beads were then washed twice in PBS with a magnetic particle concentrator. The buffer solution was aspirated and the Dynabeads again diluted in 40 ml of PBS to obtain the Dynabead solution. Enzymatic digestion solution was prepared by mixing 1 mg of collagenase enzyme (Sigma-Aldrich, Saint Louis, MO) with 1 ml of PBS solution.

Mouse kidney tissue from wild type and ACE2 KO mice (both C57BLKS/JLepr) was perfused with 40 ml Dynabeads solution injected through a cut in the left heart ventricle. The kidneys were then removed, minced and added to 50 ml of a collagenase digestion solution and put on a thermomixer (Eppendorf, Hamburg, Germany) for 30 min at 37°C with gentle agitation. The tissue was filtered twice through 100 µM strainers and centrifuged for 5 min at 900 rotations per minute. The supernatant was discarded and the remaining pellet was resuspended with 2 mL PBS solution. Glomeruli-containing Dynabeads were separated from the tubules with magnetic particle concentrators and also resuspended with PBS.

Fluorometric ACE2 and PEP Assay

The assays were performed using the fluorometric ACE2 and PEP Activity Assay kits from Bachem (Bubendorf BL, Switzerland). Kidney tissue samples were diluted to a concentration of 1µg/µl according to measurements from the BCA assay. 80 µl of a buffer solution from the kit was mixed with 10 µl of kidney tissue and 10 µl of a fluorometric substrate solution in a blackened 96-well plate. In a second set 10 µl of the specific inhibitor for ACE2 (MLN-4760) or PEP (ZPP) (both Sigma-Aldrich, St. Louis, MO, USA) was added to 10 µl substrate solution, 70 µl buffer solution and 10 µl of kidney tissue. The total volume in each setting was 100 µl. Activity was measured with a FLx800 microplate fluorescence reader (Biotek, Winooski, VT), and expressed as the difference between settings with and without the respective inhibitors.

In experiments with cultured podocytes, kidney glomeruli and tubules, the protein content of each sample was initially measured using the BCA Assay. Samples were then diluted to 1µg/µl and 10 µl of each dilution were used following the instructions described above.

BCA-Assay

The Bicinchoninic Acid Assay (Pierce, Rockford, IL) was used for quantitation of total protein in a sample. Measurements were performed in pairs on a 96-well plate. For the protein standard curve 10 µl of RIPA solution were mixed with an amount of distillated H_2O gradually decreasing from 90 µl to 40 µl from well to well. Likewise, an increasing amount of protein standard solution from 0 µl to 50 µl was added. Tissue samples were diluted 1/10 with RIPA solution and 10 µl of this mixture were added to 90 µl of distillated H_2O. Finally, 100 µl of BCA reagent were added to each well to reach a final volume of 200 µl. Results were measured on a FLx800 microplate fluorescence reader (Biotek, Winooski, VT).

Statistical Analysis

In all experiments, unless otherwise indicated, data were reported as mean ± SEM with at least three replicates per group. Pairwise comparisons were performed using two-tailed *t* test (for normally

distributed data) or Mann-Whitney test (for not normally distributed data), and a P value < 0.05 was considered significant.

Outliers were defined by a Z-Score higher than +3 or lower than -3, or a modified Z-Score of 3.5 or higher. One outlier was found for Caspase-3 activity measurements and hence the data from this cell culture generation was not taken into consideration for further evaluations. Another outlier was confirmed for APJ mRNA measurements in *db/db* mice and the value was excluded from the following calculations.

RESULTS

APJ mRNA and preproapelin mRNA in mouse kidney

The relative amount of APJ mRNA and preproapelin mRNA were evaluated using RT-qPCR in kidneys from non-diabetic *db/m* mice (*C57BLKS/JLepr*). For comparison, the mRNA levels are reported in relation to those observed in heart tissue where expression of the APJ receptor and preproapelin are known to be abundant (Medhurst *et al.*, 2003). APJ receptor mRNA levels in the kidney were clearly detectable, but only at about 1/8 of the heart mRNA (1.0±0.7 vs 7.7±1.9 AU). By contrast, preproapelin mRNA levels were not significantly different between kidney and heart (1.0±0.1 vs 1.6±0.9 AU).

Localization of APJ protein in mouse kidney

To examine which kidney cell types express APJ, immunofluorescent stained sections were evaluated by confocal microscopy in non-diabetic *db/m* mice (*C57BLKS/JLepr*). To localize APJ within the glomerulus, we utilized markers of epithelial glomerular cells (podocytes), and mesangial and endothelial glomerular cells as previously described (77). Strong colocalization was found between APJ and nephrin, a podocyte marker (Figure 3, top panel). APJ also colocalized with the podocyte marker synaptopodin, albeit not as strongly as nephrin, and weakly with podocin, another podocyte marker (Figure 3, middle panels). Double-staining with the nuclear marker WT1 also revealed some cells with APJ co-localization (Figure 3, bottom panel).

Staining of kidney glomeruli for APJ and PECAM-1 was strictly separated (Figure 4 panel A), indicating that APJ is not present in glomerular endothelial cells. Likewise, APJ showed little colocalization with the mesangial marker Desmin (Figure 4, panel B). Furthermore, no colocalization with the endothelial cell marker PECAM-1 was found in renal arteries (Figure 4, panel C). This is in concordance with absence of APJ in endothelial glomerular cells.

In renal arteries the APJ receptor colocalized with the smooth muscle marker α-SMA, reflecting its presence in the intima/ tunica media as previously described (48), but there are also areas in the vessel wall where no colocalization was seen (Figure 4, panel D).

To localize APJ within tubules, we used ACE2 and ACE as markers for proximal tubules (77) and aquaporin-2 for principal cells of the collecting tubules (Figure 5). APJ colocalized with ACE and

ACE2 (Figure 5, panels A and B respectively) showing its presence throughout the proximal tubule. APJ colocalized with aquaporin-2, albeit weakly (Figure 5C).

Studies in cultured podocytes

To localize the APJ receptor in podocytes, we used triple-label immunostaining of the APJ receptor with the introduced markers for different areas of the podocyte. Staining of cultured podocyte cells showed colocalization of APJ with all 3 podocyte markers (nephrin, synaptopodin and podocin) (Figure 6). Colocalization was equally strong, and proves expression of the receptor throughout the slit diaphragm, podocyte foot process and glomerular basement membrane. Nuclear presence of APJ was suggested by double-staining with DAPI, a nuclear marker. APJ staining was also found outside the nucleus (Figure 6).

Apelin signaling in cultured podocytes exposed to apelin 13

After showing expression of APJ in podocytes, we examined whether there is a functional role of the Apelin system in this cell type. The cellular response to Apelin-13 stimulation was determined by measuring the phosphorylation status of intracellular signaling proteins in cultured cells. Cells were stimulated with 100 nM *Pyr*^{1}Apelin-13. The ratio of phosphorylated protein to total protein was determined for AKT, p70S6K and ERK.

In podocytes, a significant transient increase in phosphorylation was seen for all three proteins (AKT, p70S6K and ERK) 15 min after stimulation (Fig. 7). After 60 min the increase subsided completely for ERK and p70S6K, and partially for AKT, showing a dynamic system of Apelin signaling activity and its deactivation, as previously shown at similar time points in other cell types (41, 42). Though the sample size in experiments with p70S6K was too low to perform a statistical analysis (n=3), the general trend of the activation pattern was similar to those of AKT and ERK.

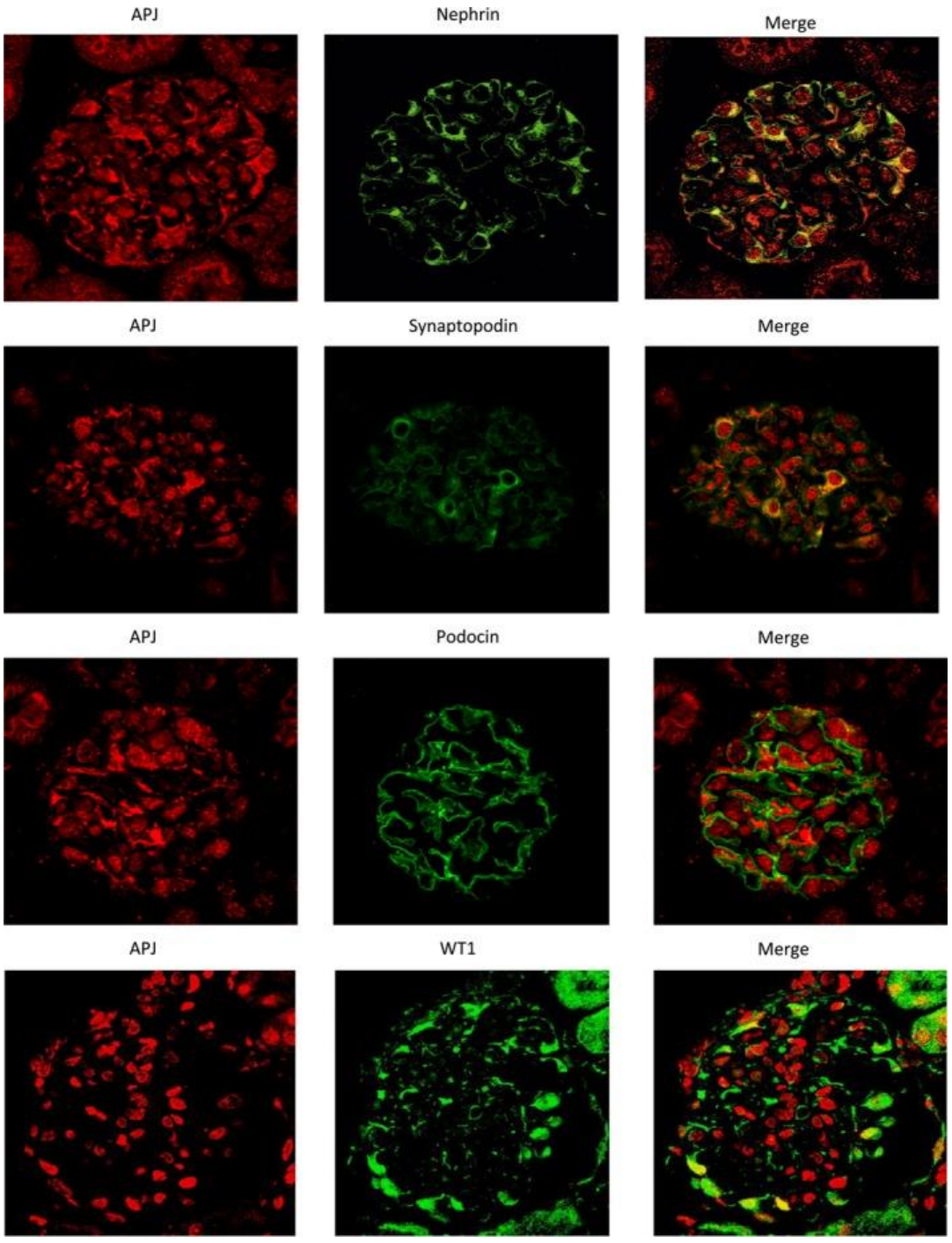

Figure 3. Immunofluorescence staining of APJ and podocyte markers in mouse kidney glomerulus

Immunofluorescence staining of APJ (red; left panels), and the podocyte markers nephrin (green; upper panel), synaptopodin (green, second panel from the top) and podocin (green, third panel from the top), in a glomerulus from a mouse kidney. APJ shows strong colocalization with nephrin (right upper panel) and synaptopodin (right second panel), and it was weaker with podocin (right third panel).

The bottom panels show staining of APJ (red; left) and the podocyte nuclear marker WT1 (green; middle). Double staining reveals APJ colocalization within WT1-positive nuclei in some podocytes (right).

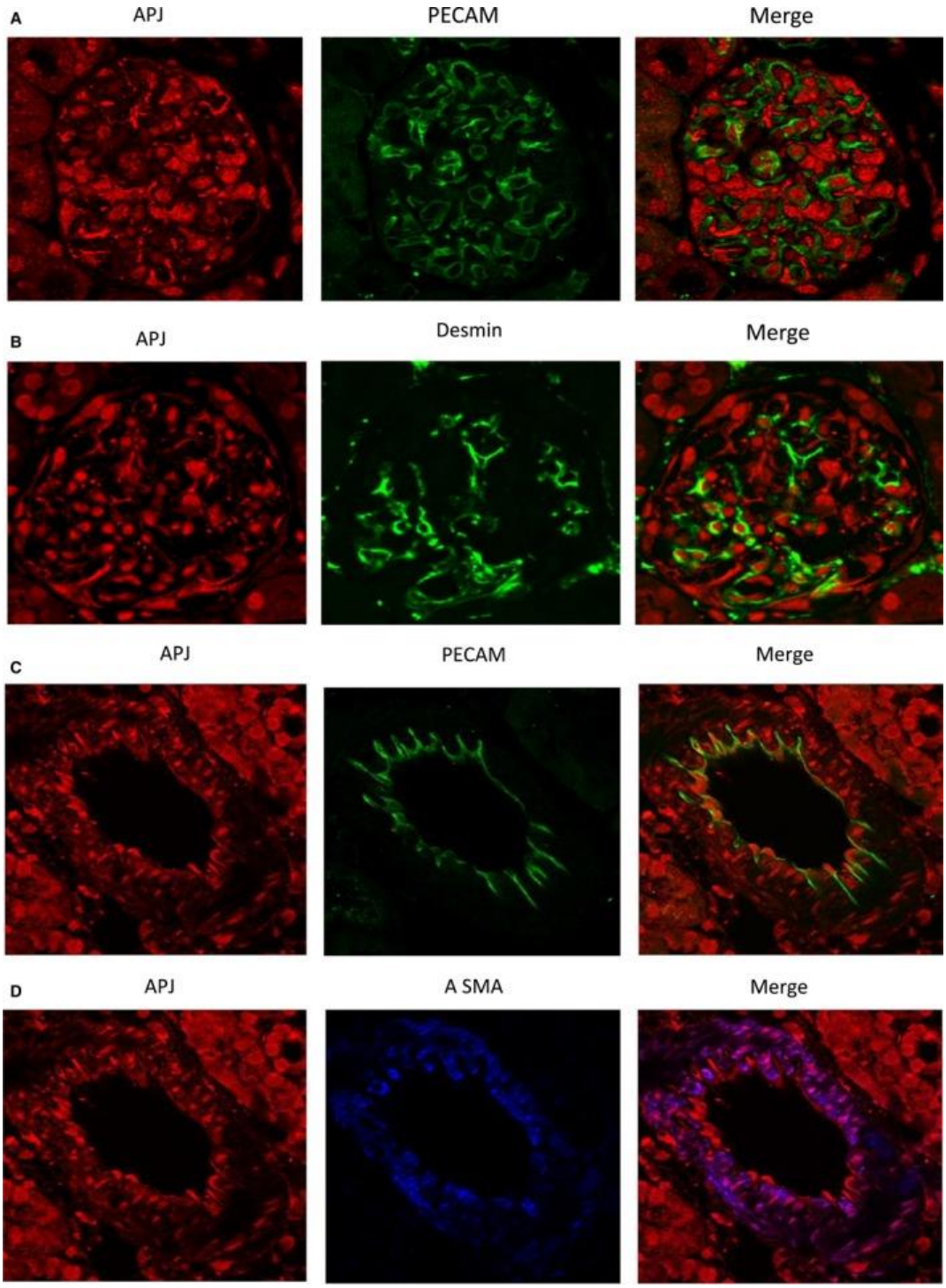

Figure 4. Immunofluorescence staining of APJ and PECAM-1, Desmin and α-SMA in mouse kidney

Immunofluorescence staining of APJ (red; left) and the endothelial cell marker, the platelet-endothelial cell adhesion molecule PECAM-1 (green; middle; A), and desmin (green, middle; B) in a kidney glomerulus. APJ shows no colocalization with PECAM-1 (right, A), and little with desmin (yellow; right, B).

Double immunofluorescence staining of APJ (red; left, C), and the endothelial cell marker platelet-endothelial cell adhesion molecule PECAM-1 (green; middle; C), and the vascular smooth muscle marker, the α-smooth

muscle actin α-SMA (blue; middle; D) in a renal vessel from mouse kidney. APJ shows no colocalization with PECAM-1 (right), but colocalizes strongly with α-SMA (pink; right).

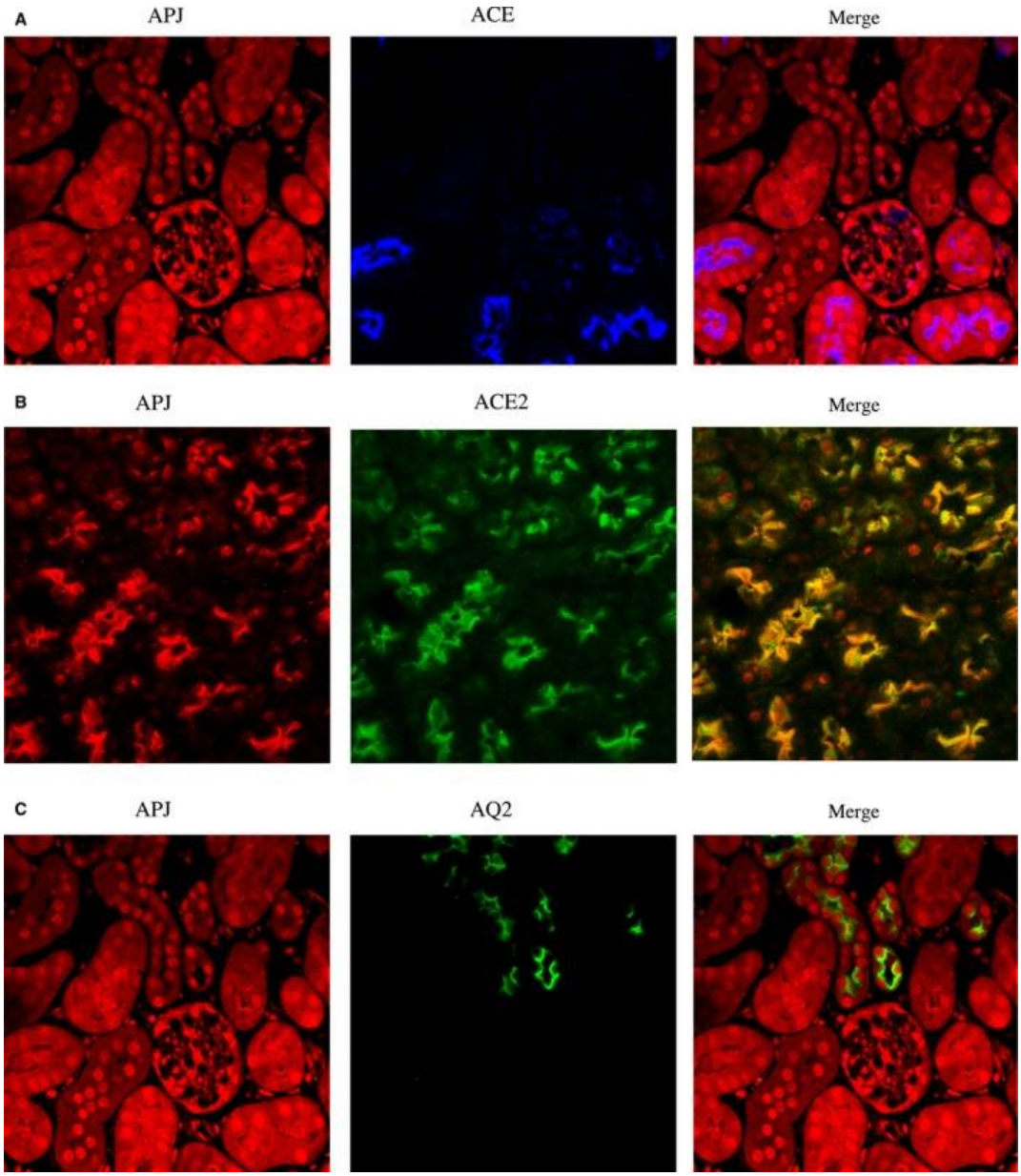

Figure 5. Immunofluorescence staining of APJ and markers for tubules in mouse kidney

Immunofluorescence double-staining of APJ (red; left) with ACE (blue; middle; A) and ACE2 (green; middle; B) in the proximal tubule (A and B), as well as with aquaporin2 (green; middle; C) in the collecting tubule (C). Images on the right are the digital overlay images (pink or yellow) for each respective row.

APJ shows strong colocalization with ACE and ACE2 throughout the proximal tubule (pink; right panel A, and yellow; right panel B). APJ is also localized in the collecting tubule, but there is very weak colocalization with aquaporin2 (panel C, right).

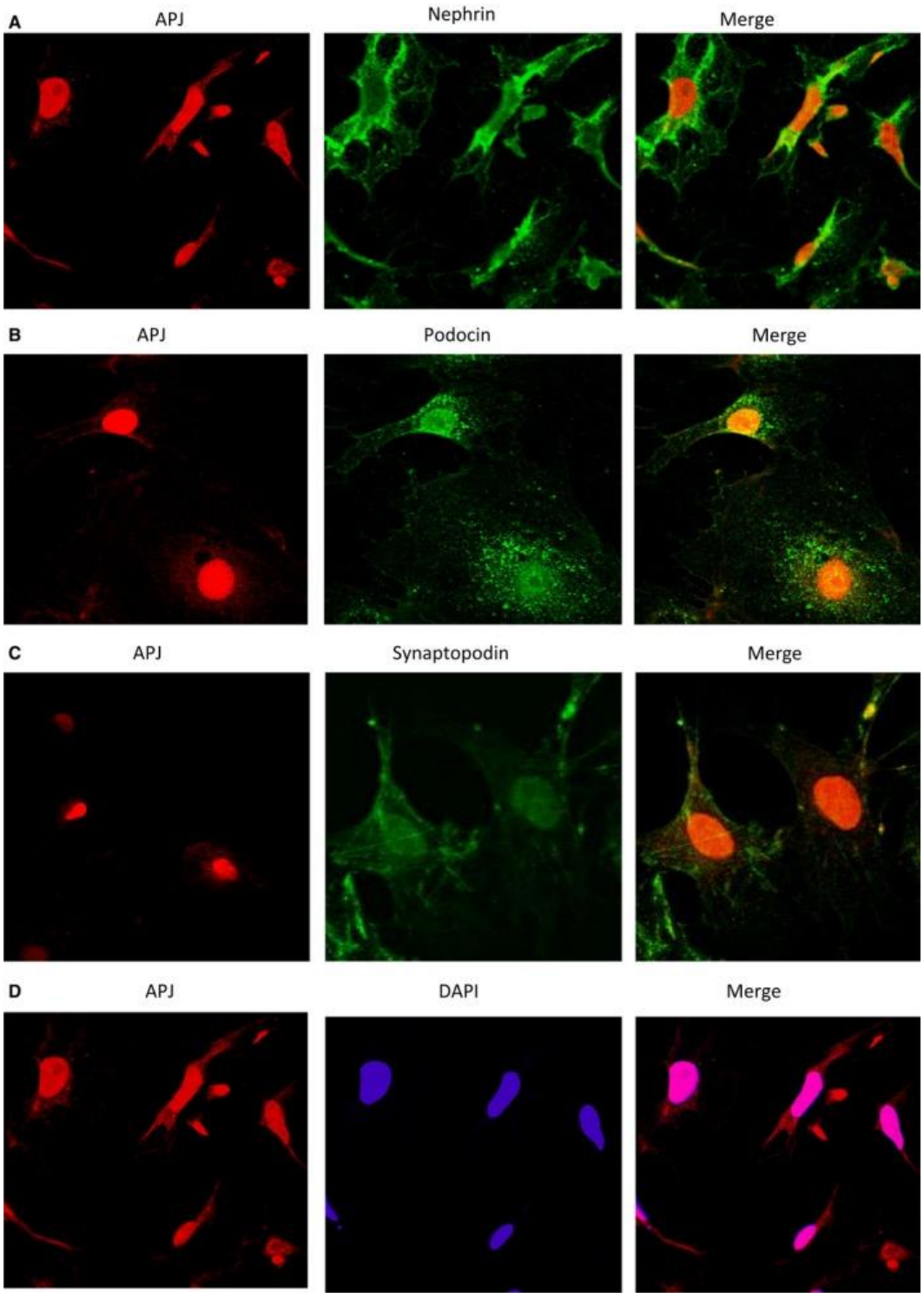

Figure 6. Triple-label immunostaining of APJ with podocyte markers and DAPI in cultured podocytes

The podocytes were triple-label immunostained with antibodies directed against APJ (red; left panels), and the podocyte markers nephrin, podocin and synaptopodin (green A through C; middle), and DAPI as a nuclear counterstain (blue; middle, D). Images on the right are the digital overlay images (yellow or pink) for each respective row. Double-staining shows colocalization of APJ with all three podocyte markers.

APJ colocalizes with a nuclear marker DAPI, but is also found outside of the nucleus (right, panel D).

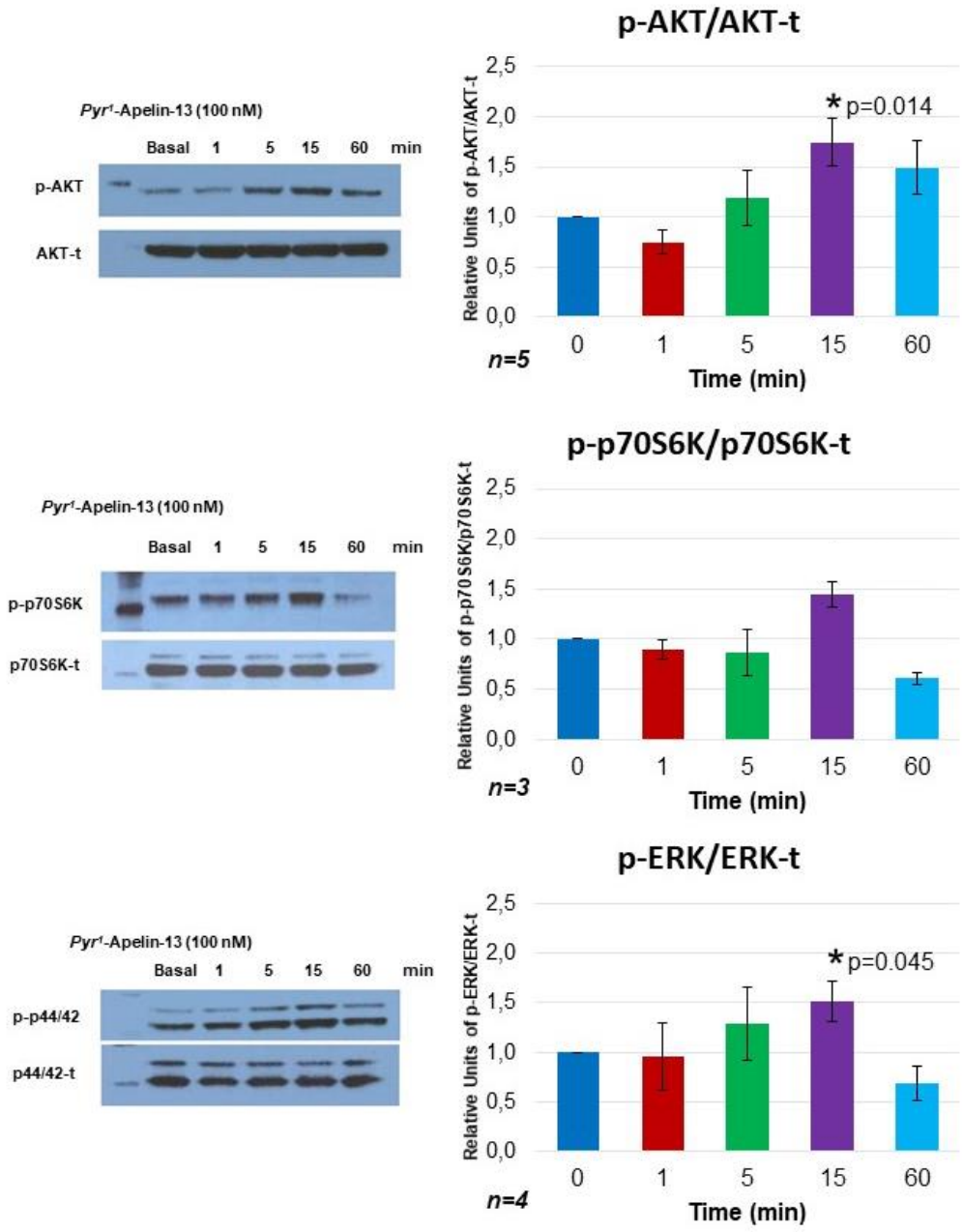

Figure 7. Time course of signaling after *Pyr*[1]Apelin-13 stimulation in podocytes

Time course of phosphorylation for AKT (top), p70S6K (middle) and ERK (bottom) after stimulation with *Pyr*[1]Apelin-13 in cultured podocytes. Significant transient increases of phosphorylated counterparts were observed in all three proteins 15 min after stimulation; suffix t – total; prefix P- phosphorylated from; The increase subsided completely after 60 min. Sample size for experiments with p70S6K was too low for statistical evaluation, albeit a similar trend was seen.

Effect of *Pyr*[1]Apelin-13 on Caspase-3 activity

AKT and ERK, the two signaling pathways that we found being activated by *Pyr*[1]Apelin 13, have been implicated in Apelin-receptor mediated suppression of apoptosis (39). We therefore examined whether *Pyr*[1]Apelin-13 exerts an anti-apoptotic effect in cultured podocytes under two glucose concentrations (11.1 mM and, 25 mM). Caspase-3 activity was significantly higher at 25 (high) than 11.1 mM (normal) glucose conditions (21722±5142 *vs* 14685±4438 RFU/µg, $p<0.05$, n=7) (Fig. 8). Caspase-3 activity in podocytes with added *Pyr*[1]Apelin-13 did not differ from activity measured without addition of *Pyr*[1]Apelin-13 (14285±3189 *vs* 14685±4438 RFU/µg, *p*=NS, n=7) (Fig. 8). Under the higher glucose concentration, however, addition of *Pyr*[1]Apelin-13 markedly decreased Caspase-3 activity (14655±3517 *vs* 21722±5142 RFU/µg, $p<0.05$, n=7).

These findings show that in cultured podocytes grown in high glucose conditions, stimulation of APJ by *Pyr*[1]Apelin-13 reduces the pro-apoptotic effect of excessive glucose.

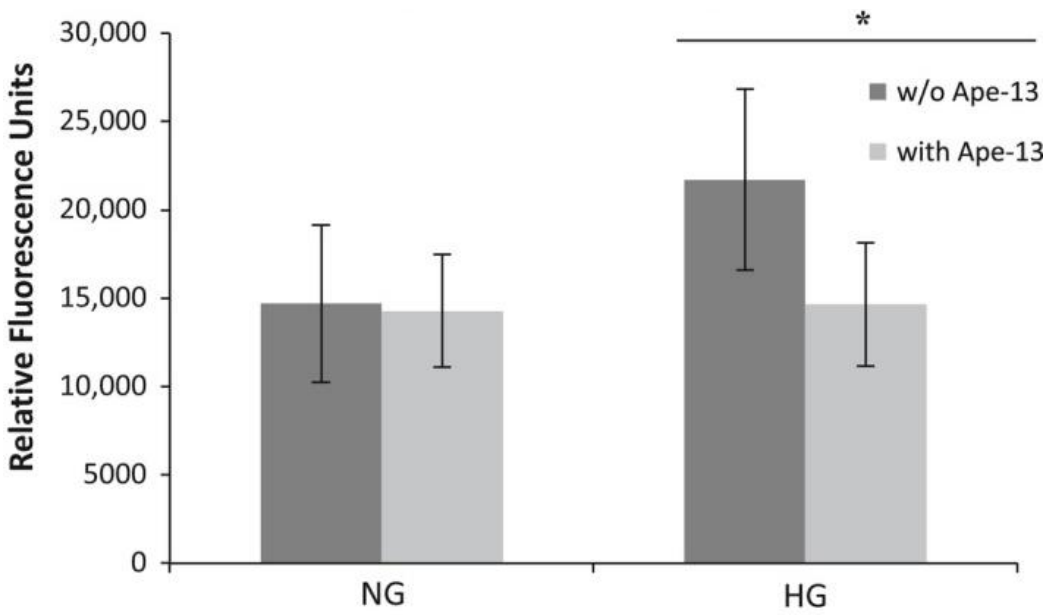

Figure 8. Caspase-3 activity in cultured podocytes

Caspase-3 activity measured in cultured podocytes in normal glucose (NG) or high glucose medium (HG) with *Pyr*[1]Apelin-13 (light grey, with Ape-13), or without addition of *Pyr*[1]apelin-13 (dark grey, w/o Ape-13). Caspase-3 activity was significantly increased in the high glucose environment. Addition of *Pyr*[1]apelin-13 to cells kept in HG medium decreased activity levels down to levels measured in the NG environment. * $p<0.05$, n=7 experiments per group.

Effect of *Pyr*[1]Apelin-13 on NADPH activity

Using the NADPH activity assay as a marker for free radical production, we sought to examine antioxidative effects of the apelinergic system on cultured cells under normal and high glucose conditions (beyond upregulation of antioxidative enzymes). NADPH activity was significantly higher with 25 (high) than 11.1 mM (normal) glucose conditions (906±107 *vs* 531±117 RFU/µg, $p<0.05$, n=6). Again, addition of *Pyr*[1]Apelin-13 to the high glucose setting decreased activity to levels measured under normal glucose (614±157 *vs* 531±117 RFU/µg, *p*=NS, n=6). However, comparison of NADPH activity measured in podocytes under normal glucose conditions with and without *Pyr*[1]Apelin-13 also showed an increase in activity with addition of *Pyr*[1]Apelin-13 (938±101 *vs* 531±117 RFU/µg, $p<0.05$, n=6). These findings may suggest a complex interaction of the apelinergic system with oxidative and antioxidative enzymes, depending on a physiological or pathological state of the studied tissue.

Effect of high glucose environment and Ang II on *APJ* and preproapelin mRNA expression

RT-qPCR of cultured podocytes revealed that an HG environment by itself significantly decreased APJ mRNA (1.19±0.26 *vs* 0.56±0.11, p<0,05) (Fig. 9). Preproapelin mRNA also decreased, but not significantly (1.30±0.24 vs 0.99±0.13, p>0.05) (Fig. 9).

Exposure to 0.1 µM Ang II for 24h significantly decreased the expression of both APJ and preproapelin mRNA under high glucose conditions, compared to podocytes cultured in a normoglycemic environment (APJ: 1.19±0.26 vs 0.16±0.05, p<0.01; Preproapelin: 1.30±0.24 vs 0.51±0.12, p<0.05). The decrease in APJ and preproapelin expression in an environment with elevated glucose and Ang II levels was also significantly higher compared to high glucose conditions alone (APJ: 0.56±0.11 vs 0.16±0.05, p<0.05; Preproapelin: 0.99±0.13 vs 0.51±0.12, p<0.05). The addition of Ang II achieved a further decrease of APJ and preproapelin mRNA than measured by high glucose conditions alone, demonstrating a downregulating effect for both Ang II and high glucose levels, which may exert a synergistic effect on the apelin system when combined.

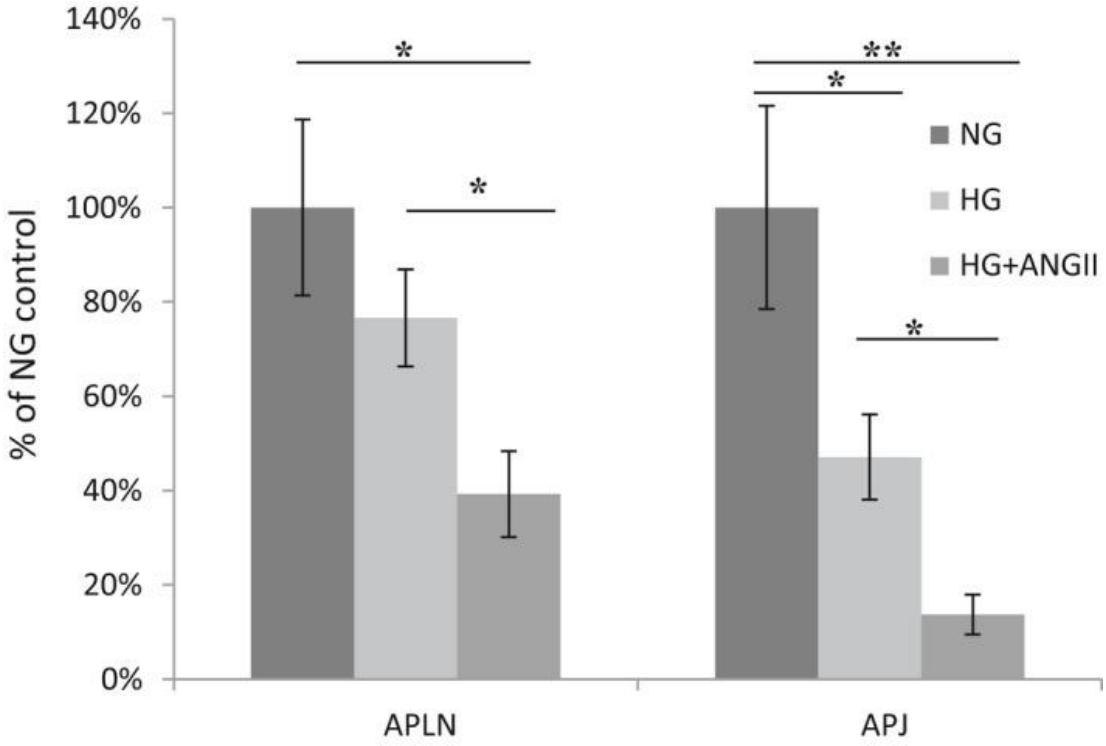

Figure 9. Environmental influence on mRNA levels of preproapelin and APJ in cultured podocytes

Relative mRNA levels of preproapelin (APLN, left) and APJ (right) in cultured podocytes in normal glucose medium (NG), high glucose medium (HG), or high glucose medium with 0.1 µM of Ang II (HG+ANGII). APJ mRNA was significantly decreased by HG, whereas preproapelin decreased, but not significantly. Both APJ and preproapelin decreased significantly under HG with addition of Ang II; * $p<0.05$; ** $p<0.01$; $n \geq 5$ for all experiments respectively.

General and light microscopy findings in *db/db* mice

These studies were performed in mice of 24-32 weeks of age. Blood sugar of *db/db* mice at this time point was significantly increased as compared to the *db/m* model. Urinary albumin in *db/db* mice was significantly increased in comparison to non-diabetic *db/m* controls (Table 3). Body weight and kidney weight were increased in *db/db* mice, but the ratio of kidneys/body weight was decreased in *db/db* mice as compared to *db/m* controls, reflecting the profound obesity of the *db/db* animals.

Table 3: **Characteristics of *db/m* and *db/db* mice at 24-32 weeks of age**

	db/m	***db/db***
Blood glucose (mmol/L)	163±9	530±41
Body weight (g)	27.8±0.5	49.5±2.0*
Kidney weight (mg)	154±9	206±6*
Ratio kidneys/body weight (mg/g)	5.6±0.4	4.2±0.2*
Albumin/Creatinine ratio (μg/mg)	7.3±2.0 (5)	613.3±366.0* (5)
Mesangial matrix expansion	0.60±0.24 (5)	2.20±0.20* (5)
Glomerular cellularity	0.6±0.24 (5)	1.8±0.20* (5)
Glomerular tuft area (μm^2)	2804.2± 111 (5)	3931.5±252.6* (5)
Podocyte count (per glomerulus)	13.1±0.3 (8)	10.0±0.4* (8)

db/m control mice; *db/db* diabetic mice (n=7 and n=6 respectively, unless stated otherwise); Data are expressed as mean ± SE. *$p < 0.05$ *db/m* vs *db/db* mice by Mann-Whitney test. Optical histology: mesangial matrix expansion and glomerular cellularity were evaluated on H&E and PAS sections by a renal pathologist. Podocyte count was performed by counting WT-1 stained nuclei in a blinded fashion by 2 independent investigators.

APJ mRNA, protein abundance and immunohistochemistry in *db/db* mice

APJ mRNA levels were first measured in diabetic *db/db* mice in whole kidney extracts by RT-qPCR. Compared to *db/m* controls of the same age (8 weeks), APJ mRNA levels were markedly decreased in *db/db* mice (1.0± 0.076 *vs* ± 0.36± 0.029, n=7, $p < 0.01$) (Fig. 10A). In western blotting, the relative protein abundance of APJ was also markedly decreased in diabetic *db/db* mice as compared to *db/m* controls (Fig. 10B).

In the immunohistochemistry, tubular APJ was also decreased in *db/db* mice compared to non-diabetic *db/m* controls (1.2±0.1 vs 1.6±0.1, $p < 0.05$) (Figure 10C). APJ stained weaker in glomerular tufts, and a significant difference could not be found between *db/db* and *db/m* (1.77±0.03 vs 1.82±0.03, respectively p=0.2).

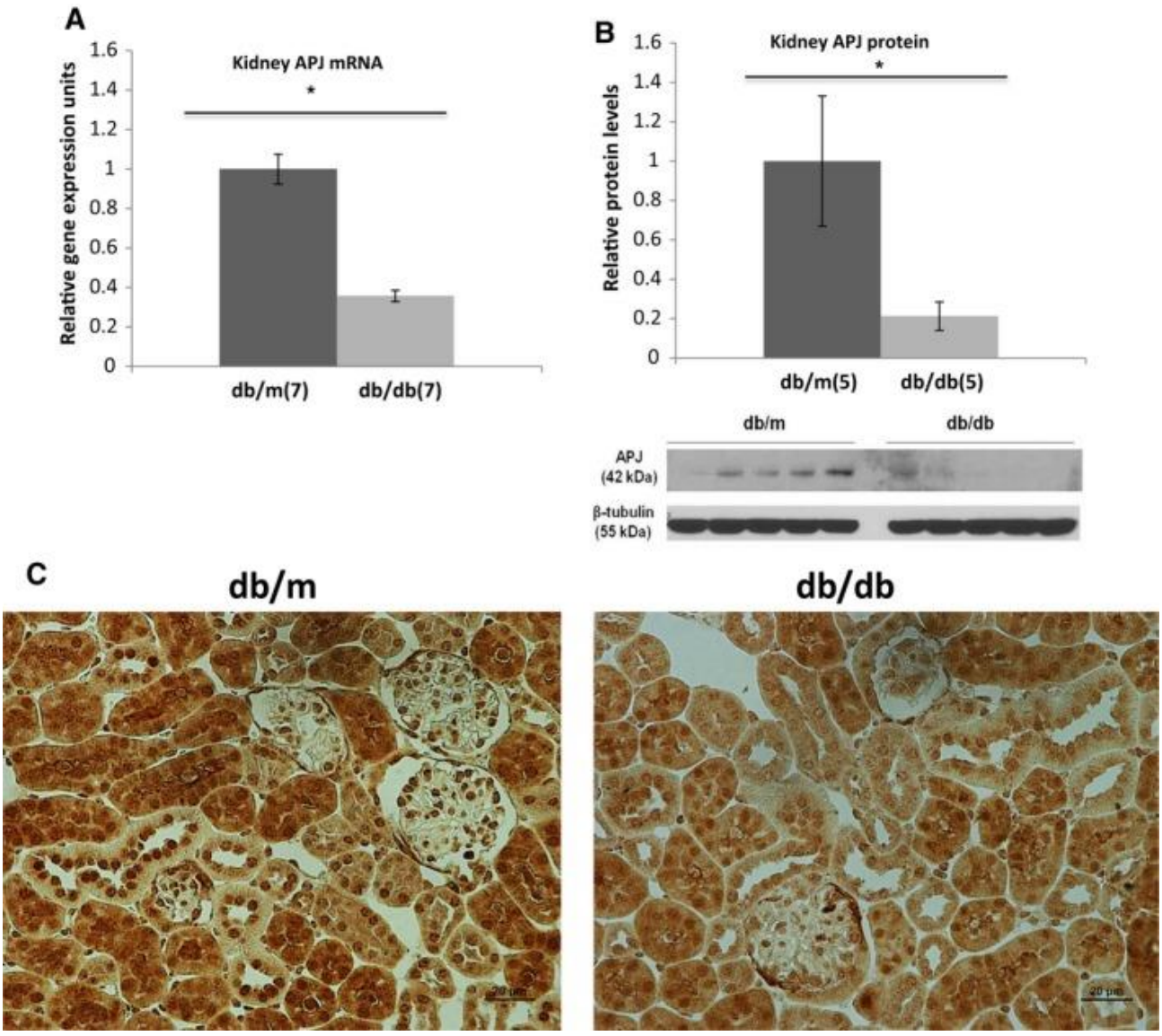

Figure 10. mRNA, protein levels and histological comparison of APJ in *db/m* and *db/db* kidney tissue

mRNA (A) and protein levels of APJ receptor by western blot (B) in whole kidney extracts of *db/m* and *db/db* mice. APJ receptor protein (42 kD) was normalized to the mouse β-tubulin (55 kD) (B). APJ mRNA and protein levels are significantly decreased in *db/db* mice. The bar graphs represent mean ± SEM values; * $p<0.05$ vs *db/m* mice.

Immunohistochemistry (C) of kidney sections from *db/m* (left) and *db/db* (right). APJ staining (dark brown) is seen in tubules and to a lesser extent in glomeruli. Staining was stronger in *db/m* as compared to *db/db* mice.

Preproapelin mRNA in the kidney and plasma apelin levels

When compared to *db/m* controls, mRNA levels of preproapelin were markedly decreased in kidneys from *db/db* mice (0.12±0.016 *vs* 1.0±0.13 AU, *n*=8, $p < 0.01$).

Apelin-12 was increased in plasma from *db/db* mice when compared to *db/m* controls (1.241±0.175 *vs* 0.786±0.072 ng/ml, *n*=6, $p < 0.05$). Apelin-12 in the urine from *db/db* mice was also increased when compared to *db/m* (1115.0±323 vs 504.4±319 pg/mg creatinine, n=12 for *db/db* and n=8 for *db/m*), although this difference did not reach statistical significance ($p = 0.054$, calculation was performed using the Mann-Whitney-U Test for not normally distributed variables).

Urine Angiotensinogen and Ang II in *db/db* mice

In *db/db* mice of 8 weeks of age, urine Ang II (normalized by urine creatinine) was significantly higher when compared with *db/m* (203±54 vs 45±13 *vs* pg/mg creatinine, $p<0.05$). Angiotensinogen (AOG) concentration normalized by creatinine was also significantly higher in *db/db* mice than in *db/m* controls (41.2±9.7 *vs* 5.9±1.7 pg/mg creatinine, $p<0.05$). Both may be attributed to an activation of the local kidney renin-angiotensin system in diabetic mouse models (70). The albumin/creatinine ratio was significantly higher in *db/db* than in *db/m* controls (303.4 ±32.1, n=25 *vs* 87.3 ± 4.3 µg/mg, n=15 respectively, $p < 0.01$).

Effect of Telmisartan on APJ in *db/db* kidney

Kidney APJ mRNA expression in *db/db* mice treated with telmisartan for 11 weeks was significantly higher as compared to untreated *db/db* mice (2.48±0.51 vs 0.95±0.16 AU, n=6 both groups, $p < 0.01$) (Fig.11). Kidney preproapelin mRNA was also significantly increased in kidneys from mice treated with telmisartan (5.41±1.51 vs 0.83±0.11 AU, n=6 both groups, $p < 0.05$) (Fig. 11).

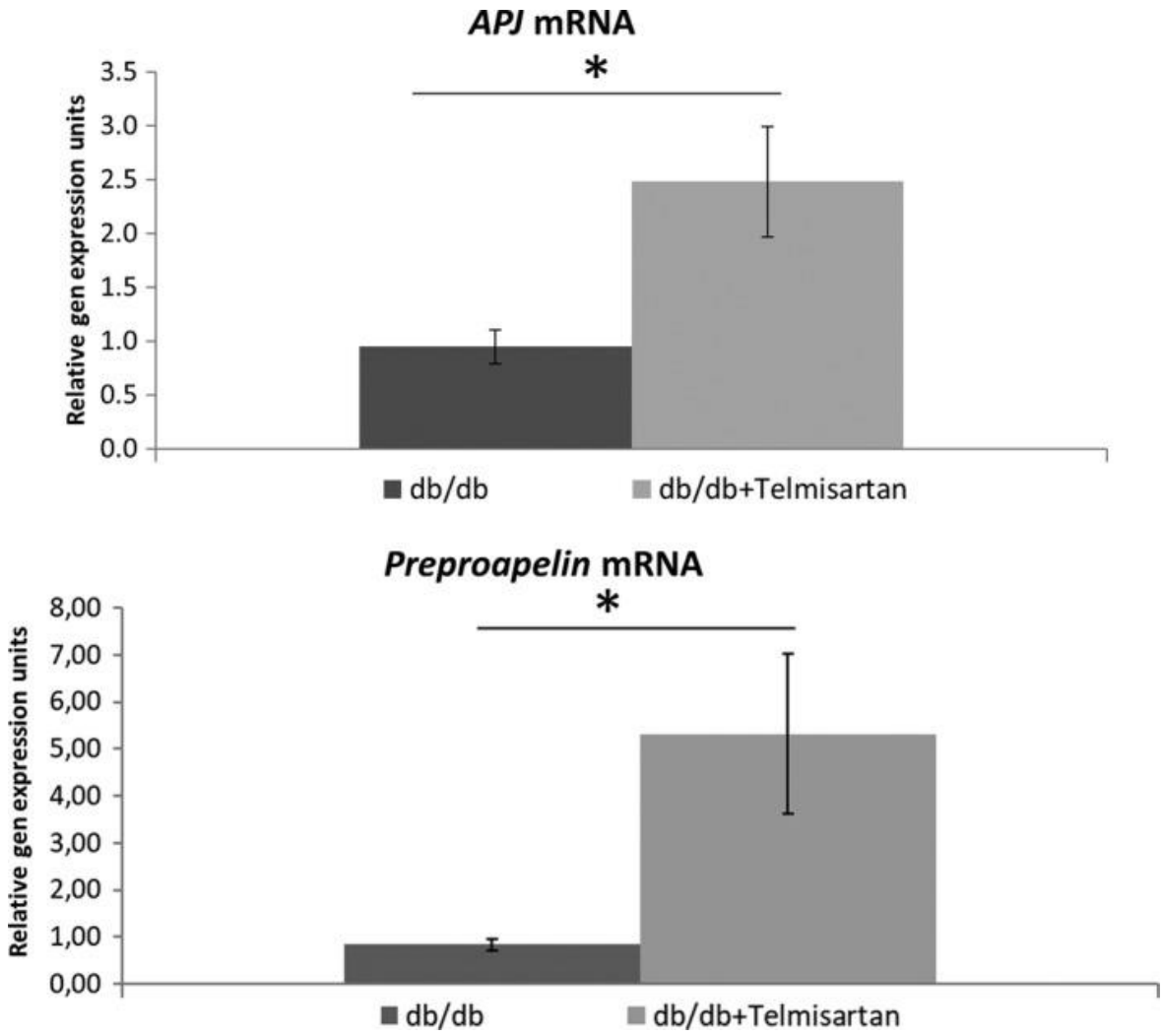

Figure 11. Influence of Telmisartan on mRNA levels of APJ and preproapelin in *db/db* kidneyFehler! Textmarke nicht definiert. **tissue**

mRNA of APJ and preproapelin measured by RT PCR in kidney lysates from untreated *db/db* mice and *db/db* mice given telmisartan, a specific AT1 blocker for 11 weeks (n=6 per group); * $p<0.05$

Apelin degradation in kidney glomeruli and tubules

Having shown the presence of the APJ-apelin system in mouse kidneys by microscopy in both glomerulus and tubules, we sought to evaluate *ex vivo* in glomerular and tubular kidney preparations carboxypeptidase enzymes that degrade Apelin-13. It has been previously established that Apelin-13 is cleaved at the N-terminus by Angiotensin-Converting-Enzyme 2 (ACE2) (65). The byproduct of this reaction is Phenylalanine, which is measurable by the Phenylalanine-Assay, thus allowing quantitative comparisons. Comparisons of human- (hr) and mouse-recombinant (mr) ACE2 showed

no significant differences in measured fluorescence units (2094±490 vs 1670±163 RFU/10µg, p=NS, n=4) (Figure 12A). Experiments with Prolylendopeptidase (PEP), another enzyme vastly expressed throughout the kidney (44), also showed enzymatic activity, which was significantly lower compared to the recombinant ACE2 enzymes (122±17 RFU/10µg, $p<0.001$ for hrACE2 and mrACE2 respectively, n=4)(Figure 12A).

In kidney tissue, enzymatic Phenylalanine cleavage was not significantly different between glomeruli and tubules (2484±568 vs 2058±567 RFU/µg, p=NS, n=4). In the presence of the specific ACE2 inhibitor MLN-4760, Phenylalanine formation was significantly reduced (2484±568 vs 935±127 RFU/µg, $p<0.05$, n=4) in glomeruli, and also in tubules, though not significantly (2058±567 vs 496±41 RFU/µg, p=0.06, n=4). Reduction of Apelin-13 cleavage by the PEP-specific inhibitor ZPP was not significant for either glomeruli or tubules. Activity measured in ACE2-KO was significantly decreased as compared to the wild type counterparts in both glomeruli (2484±568 vs 743±110 RFU/µg, $p<0.05$, n=4) and tubules (2058±567 vs 37±34 RFU/µg, $p<0.01$, n=4)(Fig. 12B). The addition of ZPP to the KO setting again did not result in a significant reduction of phenylalanine activity. Interestingly, almost no fluorometric activity was measured in KO tubules, whereas in the wild type setting the specific inhibitor MLN-4760 led to a strong but not total decrease.

The findings suggest that ACE2 is the dominant Apelin-13 degrading enzyme in the mouse kidney, whereas PEP seems to have a solely minor Apelin-13 degrading function. Based on activity measured in ACE2-KO tubules, we conclude that the degrading capacity in tubules lays solely with ACE2. In kidney glomeruli, further enzymes seem to have the ability of C-terminal Phenylalanine cleavage. The presence of ACE2 and PEP in kidney glomeruli and tubules was confirmed functionally by the respective activity assays as described above. No ACE2 activity was found in the ACE2-KO samples.

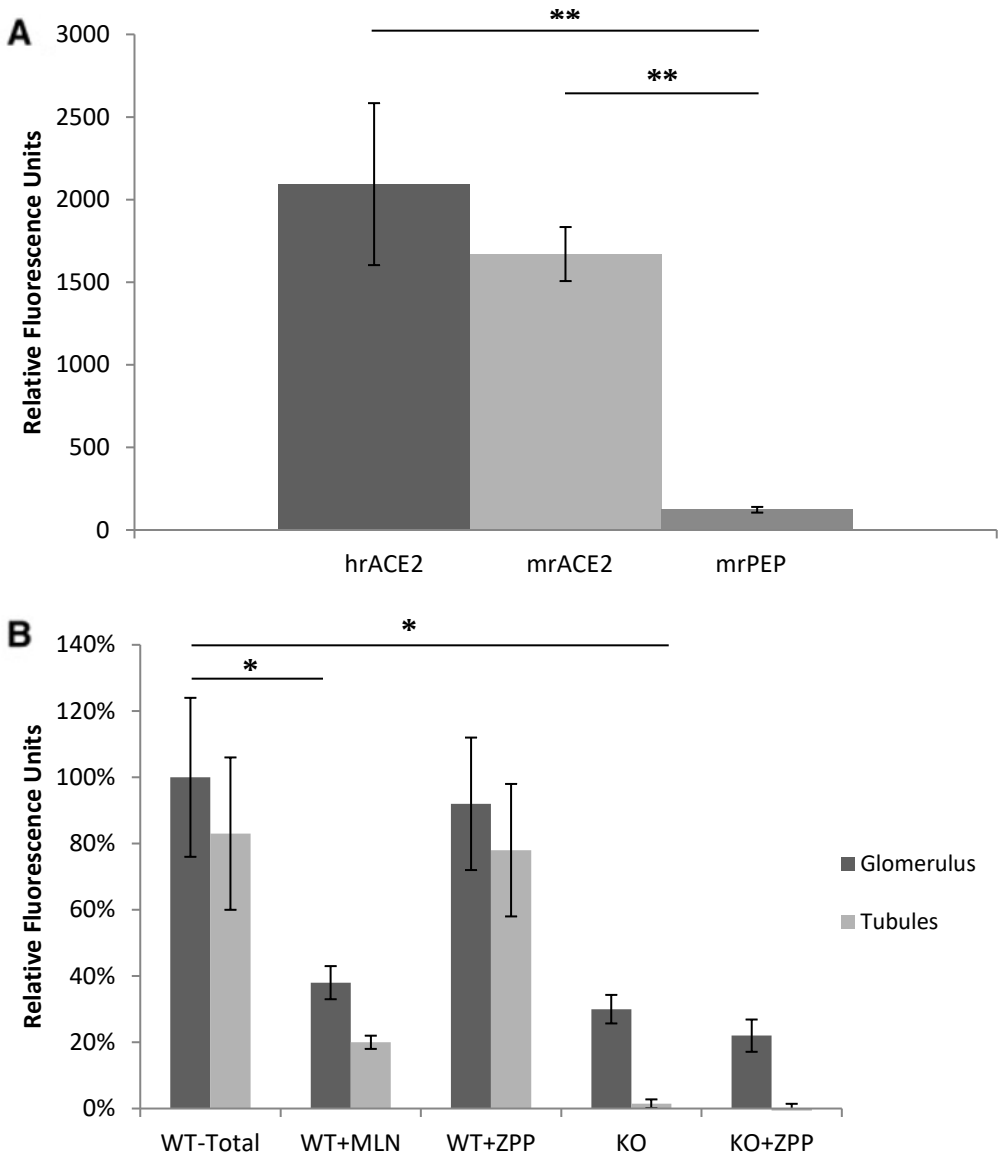

Figure 12. Comparison of C-terminal Phenylalanine cleavage by enzymes and kidney tissue

Quantitative comparison (A) of C-terminal Phenylalanine cleavage from Apelin-13 by human- and mouse-recombinant ACE2 and mouse-recombinant PEP (A). All tested enzymes were able to degrade Apelin-13. While no significant difference was found between hrACE2 and mrACE2, both showed significantly higher degradation capacity than mrPEP.

Relative Phenylalanine activity (B) measured in mouse kidney glomeruli and tubules of wild types and ACE2-KO mice incubated with only with Apelin-13 (Total), or Apelin-13 with inhibitors for ACE2 (MLN-4760) or PEP (ZPP), compared to total activity measured in wild type glomeruli. No significant difference was found between kidney glomeruli and tubules. MLN-4760 led to a significant decrease in glomeruli, but not tubules. Activity in KO tissue was significantly lower in both glomeruli and tubules. No significant decrease was achieved with ZPP in either setting. * $p<0.05$, n=4 experiments per group

Effect of high glucose environment on ACE2 and PEP activity

The observed downregulation of APJ and preproapelin mRNA in a high glucose environment is in accordance with findings in mice with Type 2 Diabetes Mellitus (8). It was established that both ACE2 and PEP are capable of cleaving the C-terminal phenylalanine residue from Apelin-13. Fluorometric ACE2 and PEP assays were performed with glomerular epithelial cells (podocytes) cultured in the previously mentioned normal glucose or high glucose conditions. PEP activity measured in podocytes in high glucose conditions was decreased compared to activity found in podocytes in the low glucose environment (1535±110 vs 1889±87 RFU/µg, $p<0,05$, $n=5$). Surprisingly, no ACE2 activity was measured in the cultured podocytes in the low or high glucose condition. This might be attributed to a mutation in the passaging of the cell lines. However, previous studies have demonstrated a downregulatory effect on glomerular ACE2 levels in DKD (56).

DISCUSSION

In this thesis, we examined the distribution of APJ in the kidney and have demonstrated that within the glomerulus the receptor is localized in epithelial glomerular cells (podocytes), but not in glomerular endothelial cells, and only very weakly in mesangial cells. Furthermore, APJ was also abundantly present in proximal tubules and renal vasculature, as previously described (46), but was only very weakly found in collecting tubules. In diabetic *db/db* mice, we found that the overall expression of APJ was depressed at the mRNA level and also at the protein level, both by western blot and by immunohistochemistry.

Using immunostaining with cultured podocytes APJ was found to colocalize with the podocyte markers nephrin, synaptopodin and podocin. Therefore, we conclude that expression of the apelin receptor was found abundantly throughout the slit diaphragm, podocyte foot process and glomerular basement membrane. Interestingly, within the podocytes the expression pattern was both nuclear as well as in the plasma membrane, as expected for a G-coupled receptor (33). By using immunocytochemical staining Lee, Lança, Cheng, Nguyen, Ji, Gobeil, Chemtob, George and O'Dowd (33) were also able to demonstrate nuclear and plasmatic localization of APJ in the human cerebellum and hypothalamus. The authors further describe APJ to be predominantly found in the nucleus, and hypothesize that the distribution pattern is indicative for receptor internalization and nuclear translocation of the receptor through nuclear pore complexes. In order for nuclear import proteins to bind and internalize APJ, a signal sequence is needed. This sequence was found in a RKRRR motif in APJ's third intracellular loop (33). Mutation of the signal sequence led to a dramatic reduction of nuclear localization. The authors therefore conclude that nuclear localization of the apelin receptor is also found to be agonist-independent to a certain degree. However, to date, the physiological implications of APJ and other G-coupled receptors in the nucleus remain unknown. It is especially noteworthy that expression of APJ was found in the slit diaphragm, podocyte foot process and glomerular basement membrane, as these are important structures for the glomerular filtration barrier and are not very permeable under physiological conditions (8). In diabetes and DKD, however, significant dysfunction of these areas and other parts of the nephron are described ultimately leading to an increased permeability resulting in the development and progress of albuminuria, respectively. Reversing these changes is seen as a possible way of promoting regression of albuminuria and restoring kidney function (62).

In the cultured podocytes, *Pyr*[1]Apelin-13 stimulated APJ triggering the activation of AKT, ERK and p70S6K pathways. The pattern of activation by apelin was brief and transient, as previously described in other cell types, such as smooth muscle cells, neurons, adipocytes and osteoblasts (3). Activation reflected by phosphorylation status of the respective proteins peaked after 15 minutes and subsided afterwards continuously until reaching initial values at less than 60 minutes. The three pathways have been described to be involved in metabolic functions as well as overall cell survival, cell proliferation and migration (3). The AKT pathway has been described to activate endothelial nitric oxide synthase (eNOS), which is responsible for the vasodilatory effect of Apelin in vessels (23, 24). Furthermore, AKT activation is associated with increased glucose uptake in skeletal muscle cells, which contributes to the beneficial effects of Apelin in Diabetes Mellitus (16). Activation of these signaling chains could also account for the protective effects attributed to the apelinergic system in DKD and diabetic cardiomyopathy. Importantly, in the study by Day, Cavaglieri and Feliers (8) administration of Apelin-13 to diabetic mice ameliorated DKD and upregulated kidney APJ. Treatment was seen to stop the progression of kidney hypertrophy, as well as to reduce glomerular hypertrophy through decreased glomerular enlargement and mesangial matrix deposition. Albuminuria was found to be ameliorated after a prolonged treatment of 6 months with Apelin-13. Taking into account the localization of APJ in podocytes and Caspase-3 suppression by Apelin-13 in these cells, it is likely that stimulation of a podocyte apelinergic system accounts, at least in part, for the reported beneficial effects of this peptide in DKD. However, it should be noted that beneficial as well as adverse effects are attributed to the Apelin-APJ axis. In Diabetes Mellitus a severe retinal complication is diabetic retinopathy, which can be divided into proliferative and non-proliferative diabetic retinopathy (PDR and NPDR). PDR development is regarded as being caused by abnormal release of angiogenic growth factors such as VEGF, which, among other things, is associated with APJ activation. Studies have shown that apelin levels in plasma as well as in vitreous are markedly elevated in patients with Diabetes Mellitus Type II and PDR, which is backed up by findings in diabetic rats (16). The partial antagonist Apelin-F13A was shown to reverse diabetes-induced retinal changes, and ameliorate the elevated levels of angiogenic factors in the retina (16). In summary, in most cases Apelin and APJ have been found to exert beneficial effects in Diabetes Mellitus and to ameliorate diabetes-induced complications with the exception of diabetic retinopathy. Due to this complexity of the apelinergic system, further research is needed to achieve favourable effects when using APJ agonists or antagonists as possible future therapeutic approaches. These substrates have to be further investigated

systematically, as much of the currently published research was performed *in vitro* on cultured cells, and has to be transferred to the animal and human model.

Apelin signaling is likely to be terminated by cleavage of the terminal Phe residue (66). Using the Phenylalanine-Assay, we were able to confirm that ACE2 is very potent in C-terminal degradation of Apelin-13 (65). A novel finding is that PEP was also found to be able to cleave Phe, but to a much lesser extent than ACE2. Presence of these two enzymes in kidney glomeruli and tubules was confirmed using the respective fluorometric activity assays, and is consistent with current literature (77). No difference in Phe-Activity was measured between kidney glomeruli and tubules. Adding the PEP specific inhibitor ZPP to kidney tissue did not lead to a significant decrease in any experimental setting with wild type or ACE2-KO renal tissue. Activity measured in kidney tubules and glomeruli was markedly decreased by the addition of the ACE2 specific inhibitor MLN-4760. For confirmation, measurements were also performed in ACE2-KO tissue. In kidney glomeruli inhibition or absence of ACE2 resulted in a similarly strong decline in Phe-Activity. In both wild type and KO tissue residual activity was found. In kidney tubules, inhibition of ACE2 also resulted in a sharp decline with measurable residual activity, whereas in ACE2-KO tissue no Phe-activity was found. This difference might be due to incomplete inhibition in the tubular setting. We therefore conclude the presence of other Apelin-degrading enzymes in kidney glomeruli apart from ACE2 and PEP. In kidney tubules, C-terminal Apelin-13 degradation is solely based on ACE2, based on results found in KO tissue.

We also found that apoptosis through activation of Caspase-3 was increased in podocytes when they were exposed to a high glucose environment, confirming the data reported by Langer *et al.* (31). We used Caspase-3 activity as a marker of podocyte apoptosis, which is considered as an early manifestation of diabetic lesions in kidneys from mouse models, such as *db/db* (58). Here, we show for the first time that stimulation by *Pyr*^{1}Apelin-13 leads to a reduction of the otherwise elevated Caspase-3 activity in a high glucose environment in podocytes (Fig. 8). This decrease in Caspase-3 activity in podocytes by *Pyr*^{1}Apelin-13 is in accordance with similar anti-apoptotic effects of the peptide in human and mouse osteoblasts (60, 72), rat cardiomyocytes (81) and rat brain tissue (27). In the normoglycemic environment, addition of *Pyr*^{1}Apelin-13 did not lead to any changes in Caspase-3 activity. This finding is in accordance with previous studies, which have shown that Apelin affects cell survival by directly suppressing apoptosis (39). Together with activation of antioxidant enzymes like catalase (45), reduction of Caspase-3 activity may partially account for the renoprotective effect of the apelinergic system in DKD, which was previously reported by Day, Cavaglieri and Feliers (8). Oxidative stress has been shown to play a significant role in the

development of DKD (8). We additionally used the NADPH-activity Assay to account for ROS production, in order to examine the antioxidative capacity of the apelinergic system. We measured a significant increase of oxidative stress in podocytes raised under high glucose conditions, which was ameliorated by addition of *Pyr*[1]Apelin-13 to levels found in podocytes in the normal glucose environment. Interestingly, addition of *Pyr*[1]Apelin-13 to podocytes raised in the stated normoglycemic conditions was also found to increase ROS production. This could be due to an error in the experimental design, or a sign of a more complicated correlation between the apelinergic system and oxidative cell stress. Anti- or prooxidative effects could be influenced by other conditions inside and outside of the cell, or even the cell type itself. Similarly, Hashimoto *et al.* (13) found that the apelinergic system cannot generally be considered anti-oxidative. Although increased levels of Apelin are associated with less circulating proinflammatory cytokines such as IL-6, TNF-α and CRP (8), their study conducted on atherosclerosis in an APJ-KO mouse model found that the KO model had fewer atherosclerotic lesions than their APJ-expressing littermates. Furthermore, apelin stimulation led to an increase in the expression of NADPH subunits, resulting in increased oxidative stress in vascular smooth muscle cells, similar to our findings in podocytes. Conversely, APJ stimulation also leads to an activation of eNOS, which is considered to exert protective effects on the genesis of atherosclerosis (13). Upregulation of components of the apelinergic system is also discussed as being a compensatory mechanism to limit inflammation, as recent studies have found that intraperitoneal administration of TNF- α in mice increased Apelin expression in adipocytes and in the circulation (7). It appears that the implication of the apelinergic system on ROS production still remains not completely conclusive, and further studies have to be conducted. Modification of the anti-inflammatory properties of the Apelin-APJ axis could prove to be a powerful renoprotective mechanism, as recent studies have shown that NF-kB targeted anti-inflammatory approaches do improve renal function in diabetic mice (8).

In cultured podocytes, we showed that high glucose downregulates APJ mRNA levels, and this effect is markedly accentuated by exposure to Ang II (Fig. 9). These findings prompted us to study the effect of diabetes *in vivo* on kidney APJ expression in the *db/db* mouse model of DKD. In these animals, urinary albumin excretion was increased as previously reported (18, 54) and glomerular mesangial expansion was present, as well as an increase in the glomerular tuft area in glomeruli from both the cortex and juxtamedullary region. This was accompanied by a lower podocyte count in the diabetic mouse model. The kidneys were hypertrophic. Both kidney and glomerular hypertrophy are typically found already in early manifestations of diabetic nephropathy, and changes persist throughout disease

(8). Glomerular hypertrophy is caused by an enlargement of capillary lumina and an increase of capillary cell mass, whereas mainly tubular cell hypertrophy leads to renal hypertrophy (8). A causative role of suppressed APJ expression in the development of DKD requires further evidence, but several findings suggest its important role. The pro-apoptotic and pro-oxidative actions of high glucose, as inferred by Caspase-3 and NADPH-activity, was suppressed by the stimulation of APJ with *Pyr*^{1}Apelin-13 in cultured podocytes. We also showed that Ang II downregulates both APJ and preproapelin in podocytes exposed to high glucose.

In the db/db mouse model blood glucose levels were increased when compared to their db/m littermates at 24 weeks of age. Body and kidney weights were increased as well, though the kidney-to-body ratio was decreased, reflecting severe obesity in the diabetic mouse model. Furthermore, the albumin/creatinine ratio was elevated, a sign of damage to the kidney filtration barrier (1). Histologically, mesangial matrix expansion was found, as well as an increase in glomerular cellularity and the glomerular tuft area, and a decrease in podocyte count per glomerulus. These histological findings are in accordance with previous studies comparing diabetes-induced changes in mouse kidneys (8). In the *db/db* model, like in other models of DKD in mice and humans (49, 59, 64, 70, 71), the kidney RAS is overactive, as reflected by high levels of urinary angiotensinogen and Ang II. This upregulation is at least partially attributable to stimulation by the high-glucose environment (49, 68). Levels of Apelin in the plasma of the *db/db* mice were elevated when compared to the *db/m* mice which is in accordance with other studies (3). Concurrently, urinary Apelin levels were also found to be increased, which might be due to a combination of the elevated levels in plasma, and increased filtration caused by damage to the filtration barrier in diabetic mice. It is possible that downregulation of the local apelinergic system in the kidneys is attempted to be compensated for by general upregulation of components of the Apelin-APJ axis in the circulation and possibly other tissues. Overall, our data suggests that high glucose and high Ang II activity may converge to suppress APJ in podocytes, and contribute to the development of the glomerular lesions of DKD and its progression. Development of complications of hyperglycaemia such as DKD is especially promoted by the intrarenal renin-angiotensin system (8), and RAS overactivity was confirmed in the diabetic mice in our experiments. The apelinergic system is suggested to antagonize pathological effects of RAS overactivity, therefore the reduction in APJ and preoproapelin mRNA in the kidney could leave the activated local renin-angiotensin system unopposed, and thus could play an important role in the development of diabetic complications (3, 8). Apelin treatment in diabetic mice has been shown to

recover renal injury and renal inflammation, and upregulate APJ expression, making it a promising target for pharmaceutical intervention (8).

The suppression of APJ and preproapelin that we found in podocytes was previously described in different tissues such as adipocytes and cardiomyocytes, which was reported to be dose-dependent and mediated by the AT1-receptor (22, 69). The combination of high glucose and high levels of Ang II achieved a higher level of APJ and preproapelin downregulation than the high glucose environment alone (Fig 8). This synergistic effect may explain the observed low level of APJ observed in the *db/db* mouse model of DKD, where we found RAS overactivity at the kidney level (i.e. increased urinary AOG and Ang II). Overactivity of the kidney RAS is a feature of other models of DKD and human DKD (47, 49, 59, 64, 70, 71). Possibly downregulation of the kidney APJ is, at least in part, the consequence of hyperglycaemia and RAS overactivity at the tissue level.

Furthermore, hyperglycaemia was found to decrease activity of PEP in cultured podocytes. Interestingly, no ACE2 activity was measured, which might be due to a mutation between generations in the passaging of this set of cultured cells. Though we could not confirm a downregulatory effect on ACE2 in our experimental setting, current literature has described the similar effects of a hyperglycaemic environment on ACE2 expression (56). Since both enzymes have been found to degrade Apelin-13, downregulation could partially antagonize the decrease in APJ and preproapelin expression and therefore function as a regulatory mechanism to protect podocytes and kidney function. It should be noted that both enzymes also play important roles in metabolism and degradation of Angiotensin II (65). Hence, downregulation would lead to increased levels of certain RAS components. It remains to be seen whether downregulation of PEP and ACE2 can be attributed to a physiological response of podocytes to increase chances of survival, or whether it is due to pathological mechanisms caused by the hyperglycaemic environment itself.

Notably, specific AT1 blockade with telmisartan resulted in an increase in the APJ and preproapelin mRNA in *db/db* mice in comparison to untreated diabetic littermates after 11 weeks of treatment. In the current literature, this has previously only been described for APJ in the cardiac apelinergic system in hypertrophied hearts, and for APJ as well as Apelin in adipose tissue (22, 69). In their study, Wu, Cheng, Hao, Zhang, Yao, Murohara and Dai (69) were able to show an upregulatory effect through RAS inhibition with both the AT1-blocker olmesartan and the ACE-inhibitor perindopril. Upregulation of these two major components of the apelinergic system, APJ and preproapelin, may be yet another beneficial effect of AT1-blockers beyond AT1-inhibition.

In conclusion, we have shown that in the kidney glomerulus the apelin receptor is preferentially localized in podocytes, both nuclear and in cell plasma. Stimulation of APJ activates pathways associated with cell survival and proliferation like AKT, ERK and p70S6K. The activation pattern was found to be brief and transient. In cultured podocytes, high glucose and Ang II decrease APJ and preproapelin expression at the mRNA level. A high glucose environment was further found to exert a proapoptotic and prooxidative effect. While the apoptotic and oxidative effects of high glucose can be reversed by stimulation of APJ by one of its main ligands Apelin-13, stimulation with this ligand under normoglycemic conditions also increased oxidative stress. In diabetic *db/db* mice, kidney APJ expression was markedly decreased at the mRNA level and protein level, whereas treatment with telmisartan led to an increase in APJ and preproapelin mRNA. Altogether our findings suggest a role for APJ down-regulation in the development of DKD. The half-life of apelin-13 and other apelins is short (minutes), but with the development of apelin agonists with a prolonged half-life (17, 25), the podocyte apelinergic system may become a good target for the treatment of DKD.

REFERENCES

1. **Alicic RZ, Rooney MT, and Tuttle KR**. Diabetic Kidney Disease. *Challenges, Progress, and Possibilities* 12: 2032-2045, 2017.
2. **Cai X, Bai B, Zhang R, Wang C, and Chen J**. Apelin receptor homodimer-oligomers revealed by single-molecule imaging and novel G protein-dependent signaling. *Sci Rep* 7: 40335, 2017.
3. **Chaves-Almagro C, Castan-Laurell I, Dray C, Knauf C, Valet P, and Masri B**. Apelin receptors: From signaling to antidiabetic strategy. *European journal of pharmacology* 763: 149-159, 2015.
4. **Chen H, Li J, Jiao L, Petersen RB, Li J, Peng A, Zheng L, and Huang K**. Apelin inhibits the development of diabetic nephropathy by regulating histone acetylation in Akita mouse. *The Journal of Physiology* 592: 505-521, 2014.
5. **Chen H, Wan D, Wang L, Peng A, Xiao H, Petersen RB, Liu C, Zheng L, and Huang K**. Apelin protects against acute renal injury by inhibiting TGF-β1. *Biochimica et Biophysica Acta (BBA) - Molecular Basis of Disease* 1852: 1278-1287, 2015.
6. **Chen S, Kasama Y, Lee JS, Jim B, Marin M, and Ziyadeh FN**. Podocyte-Derived Vascular Endothelial Growth Factor Mediates the Stimulation of α3(IV) Collagen Production by Transforming Growth Factor-β1 in Mouse Podocytes. *Diabetes* 53: 2939-2949, 2004.
7. **Daviaud D, Boucher J, Gesta S, Dray C, Guigne C, Quilliot D, Ayav A, Ziegler O, Carpene C, Saulnier-Blache J-S, Valet P, and Castan-Laurell I**. TNFα up-regulates apelin expression in human and mouse adipose tissue. *The FASEB Journal* 20: 1528-1530, 2006.
8. **Day RT, Cavaglieri RC, and Feliers D**. Apelin retards the progression of diabetic nephropathy. *American Journal of Physiology - Renal Physiology* 304: F788-F800, 2013.
9. **De Mota N, Reaux-Le Goazigo A, El Messari S, Chartrel N, Roesch D, Dujardin C, Kordon C, Vaudry H, Moos F, and Llorens-Cortes C**. Apelin, a potent diuretic neuropeptide counteracting vasopressin actions through inhibition of vasopressin neuron activity and vasopressin release. *Proceedings of the National Academy of Sciences of the United States of America* 101: 10464-10469, 2004.
10. **Farkasfalvi K, Stagg MA, Coppen SR, Siedlecka U, Lee J, Soppa GK, Marczin N, Szokodi I, Yacoub MH, and Terracciano CMN**. Direct effects of apelin on cardiomyocyte contractility and electrophysiology. *Biochemical and biophysical research communications* 357: 889-895, 2007.
11. **Gurzu B, Petrescu BC, Costuleanu M, and Petrescu G**. Interactions between apelin and angiotensin II on rat portal vein. *Journal of the Renin-Angiotensin-Aldosterone System* 7: 212-216, 2006.
12. **Habata Y, Fujii R, Hosoya M, Fukusumi S, Kawamata Y, Hinuma S, Kitada C, Nishizawa N, Murosaki S, Kurokawa T, Onda H, Tatemoto K, and Fujino M**. Apelin, the natural ligand of the orphan receptor APJ, is abundantly secreted in the colostrum. *Biochimica et Biophysica Acta (BBA) - Molecular Cell Research* 1452: 25-35, 1999.
13. **Hashimoto T, Kihara M, Imai N, Yoshida S-I, Shimoyamada H, Yasuzaki H, Ishida J, Toya Y, Kiuchi Y, Hirawa N, Tamura K, Yazawa T, Kitamura H, Fukamizu A, and Umemura S**. Requirement of apelin-apelin receptor system for oxidative stress-linked atherosclerosis. *The American journal of pathology* 171: 1705-1712, 2007.
14. **Hashimoto T, Kihara M, Ishida J, Imai N, Yoshida S-i, Toya Y, Fukamizu A, Kitamura H, and Umemura S**. Apelin Stimulates Myosin Light Chain Phosphorylation in Vascular Smooth Muscle Cells. *Arteriosclerosis, Thrombosis, and Vascular Biology* 26: 1267-1272, 2006.

15. **Hosoya M, Kawamata Y, Fukusumi S, Fujii R, Habata Y, Hinuma S, Kitada C, Honda S, Kurokawa T, Onda H, Nishimura O, and Fujino M**. Molecular and Functional Characteristics of APJ: TISSUE DISTRIBUTION OF mRNA AND INTERACTION WITH THE ENDOGENOUS LIGAND APELIN. *Journal of Biological Chemistry* 275: 21061-21067, 2000.
16. **Hu H, He L, Li L, and Chen L**. Apelin/APJ system as a therapeutic target in diabetes and its complications. *Molecular Genetics and Metabolism* 119: 20-27, 2016.
17. **Huang Z, He L, Chen Z, and Chen L**. Targeting drugs to APJ receptor: From signaling to pathophysiological effects. *Journal of cellular physiology* 2018.
18. **Hummel KP, Dickie MM, and Coleman DL**. Diabetes, a New Mutafton in the Mouse. *Science* 153: 1127, 1966.
19. **Hus-Citharel A, Bouby N, Frugière A, Bodineau L, Gasc J-M, and Llorens-Cortes C**. Effect of apelin on glomerular hemodynamic function in the rat kidney. *Kidney International* 74: 486-494, 2008.
20. **Hus-Citharel A, Bouby N, Frugiere A, Bodineau L, Gasc JM, and Llorens-Cortes C**. Effect of apelin on glomerular hemodynamic function in the rat kidney. *Kidney Int* 74: 486-494, 2008.
21. **Ishida J, Hashimoto T, Hashimoto Y, Nishiwaki S, Iguchi T, Harada S, Sugaya T, Matsuzaki H, Yamamoto R, Shiota N, Okunishi H, Kihara M, Umemura S, Sugiyama F, Yagami K-i, Kasuya Y, Mochizuki N, and Fukamizu A**. Regulatory Roles for APJ, a Seven-transmembrane Receptor Related to Angiotensin-type 1 Receptor in Blood Pressure in Vivo. *Journal of Biological Chemistry* 279: 26274-26279, 2004.
22. **Iwanaga Y, Kihara Y, Takenaka H, and Kita T**. Down-regulation of cardiac apelin system in hypertrophied and failing hearts: Possible role of angiotensin II–angiotensin type 1 receptor system. *Journal of molecular and cellular cardiology* 41: 798-806, 2006.
23. **Japp AG, Cruden NL, Amer DAB, Li VKY, Goudie EB, Johnston NR, Sharma S, Neilson I, Webb DJ, Megson IL, Flapan AD, and Newby DE**. Vascular Effects of Apelin In Vivo in Man. *Journal of the American College of Cardiology* 52: 908-913, 2008.
24. **Jia YX, Lu ZF, Zhang J, Pan CS, Yang JH, Zhao J, Yu F, Duan XH, Tang CS, and Qi YF**. Apelin activates l-arginine/nitric oxide synthase/nitric oxide pathway in rat aortas. *Peptides* 28: 2023-2029, 2007.
25. **Juhl C, Els-Heindl S, Schönauer R, Redlich G, Haaf E, Wunder F, Riedl B, Burkhardt N, Beck-Sickinger AG, and Bierer D**. Development of Potent and Metabolically Stable APJ Ligands with High Therapeutic Potential. *ChemMedChem* 11: 2378-2384, 2016.
26. **Kalea AZ, and Batlle D**. Apelin and ACE2 in cardiovascular disease. *Curr Opin Investig Drugs* 11: 273-282, 2010.
27. **Khaksari M, Aboutaleb N, Nasirinezhad F, Vakili A, and Madjd Z**. Apelin-13 Protects the Brain Against Ischemic Reperfusion Injury and Cerebral Edema in a Transient Model of Focal Cerebral Ischemia. *Journal of Molecular Neuroscience* 48: 201-208, 2012.
28. **Kleinz MJ, and Davenport AP**. Immunocytochemical localization of the endogenous vasoactive peptide apelin to human vascular and endocardial endothelial cells. *Regulatory Peptides* 118: 119-125, 2004.
29. **Kleinz MJ, Skepper JN, and Davenport AP**. Immunocytochemical localisation of the apelin receptor, APJ, to human cardiomyocytes, vascular smooth muscle and endothelial cells. *Regulatory Peptides* 126: 233-240, 2005.
30. **Lambrecht NWG, Yakubov I, Zer C, and Sachs G**. Transcriptomes of purified gastric ECL and parietal cells: identification of a novel pathway regulating acid secretion. *Physiological genomics* 25: 153-165, 2006.
31. **Langer S, Kreutz R, and Eisenreich A**. Metformin modulates apoptosis and cell signaling of human podocytes under high glucose conditions. *Journal of Nephrology* 29: 765-773, 2016.

32. **Lee DK, Cheng R, Nguyen T, Fan T, Kariyawasam AP, Liu Y, Osmond DH, George SR, and O'Dowd BF**. Characterization of Apelin, the Ligand for the APJ Receptor. *Journal of neurochemistry* 74: 34-41, 2000.
33. **Lee DK, Lança AJ, Cheng R, Nguyen T, Ji XD, Gobeil F, Chemtob S, George SR, and O'Dowd BF**. Agonist-independent Nuclear Localization of the Apelin, Angiotensin AT1, and Bradykinin B2 Receptors. *Journal of Biological Chemistry* 279: 7901-7908, 2004.
34. **Lee DK, Saldivia VR, Nguyen T, Cheng R, George SR, and O'Dowd BF**. Modification of the Terminal Residue of Apelin-13 Antagonizes Its Hypotensive Action. *Endocrinology* 146: 231-236, 2005.
35. **Lee E-Y, Chung CH, Kim JH, Joung H-J, and Hong SY**. Antioxidants ameliorate the expression of vascular endothelial growth factor mediated by protein kinase C in diabetic podocytes. *Nephrology Dialysis Transplantation* 21: 1496-1503, 2006.
36. **Lee SM, and Bressler R**. Prevention of Diabetic Nephropathy by Diet Control in the db/db Mouse. *Diabetes* 30: 106-111, 1981.
37. **Li L, Zeng H, and Chen J-X**. Apelin-13 increases myocardial progenitor cells and improves repair postmyocardial infarction. *American Journal of Physiology-Heart and Circulatory Physiology* 303: H605-H618, 2012.
38. **Lin MH, Miller JB, Kikkawa Y, Suleiman HY, Tryggvason K, Hodges BL, and Miner JH**. Laminin-521 Protein Therapy for Glomerular Basement Membrane and Podocyte Abnormalities in a Model of Pierson Syndrome. *J Am Soc Nephrol* 2018.
39. **Liu J, Liu M, and Chen L**. Novel pathogenesis: regulation of apoptosis by Apelin/APJ system. *Acta Biochimica et Biophysica Sinica* 49: 471-478, 2017.
40. **Lv D, Li H, and Chen L**. Apelin and APJ, a novel critical factor and therapeutic target for atherosclerosis. *Acta Biochimica et Biophysica Sinica* 45: 527-533, 2013.
41. **Masri B, Morin N, Cornu M, Knibiehler B, and Audigier Y**. Apelin (65-77) activates p70 S6 kinase and is mitogenic for umbilical endothelial cells. *The FASEB Journal* 18: 1909-1911, 2004.
42. **Masri B, Morin N, Pedebernade L, Knibiehler B, and Audigier Y**. The Apelin Receptor Is Coupled to Gi1 or Gi2 Protein and Is Differentially Desensitized by Apelin Fragments. *Journal of Biological Chemistry* 281: 18317-18326, 2006.
43. **Medhurst AD, Jennings CA, Robbins MJ, Davis RP, Ellis C, Winborn KY, Lawrie KWM, Hervieu G, Riley G, Bolaky JE, Herrity NC, Murdock P, and Darker JG**. Pharmacological and immunohistochemical characterization of the APJ receptor and its endogenous ligand apelin. *Journal of Neurochemistry* 84: 1162-1172, 2003.
44. **Myohanen TT, Garcia-Horsman JA, Tenorio-Laranga J, and Mannisto PT**. Issues about the physiological functions of prolyl oligopeptidase based on its discordant spatial association with substrates and inconsistencies among mRNA, protein levels, and enzymatic activity. *The journal of histochemistry and cytochemistry : official journal of the Histochemistry Society* 57: 831-848, 2009.
45. **Nishida M, and Hamaoka K**. *The Apelin-APJ system: its role in renal physiology and potential therapeutic applications for renal disease*. 2013, p. 7.
46. **O'Carroll A-M, Selby TL, Palkovits M, and Lolait SJ**. Distribution of mRNA encoding B78/apj, the rat homologue of the human APJ receptor, and its endogenous ligand apelin in brain and peripheral tissues. *Biochimica et Biophysica Acta (BBA) - Gene Structure and Expression* 1492: 72-80, 2000.
47. **Patney V, Chaudhary K, and Whaley-Connell A**. Treatment of Diabetic Kidney Disease With Hypertension Control and Renin Angiotensin System Inhibition. *Advances in chronic kidney disease* 25: 158-165, 2018.

48. **Pereira V, Abidu-Figueiredo M, Pereira-Sampaio M, Chagas M, Silva Costa W, and J B Sampaio F**. *Sinusoidal Constriction and Vascular Hypertrophy in the Diabetes-Induced Rabbit Penis*. 2013, p. 424-431.
49. **Peti-Peterdi J, Kang JJ, and Toma I**. Activation of the renal renin–angiotensin system in diabetes—new concepts. *Nephrology Dialysis Transplantation* 23: 3047-3049, 2008.
50. **Rai R, Ghosh AK, Eren M, Mackie AR, Levine DC, Kim S-Y, Cedernaes J, Ramirez V, Procissi D, Smith LH, Woodruff TK, Bass J, and Vaughan DE**. Downregulation of the Apelinergic Axis Accelerates Aging, whereas Its Systemic Restoration Improves the Mammalian Healthspan. *Cell Reports* 21: 1471-1480, 2017.
51. **Roselli S, Gribouval O, Boute N, Sich M, Benessy F, Attié T, Gubler M-C, and Antignac C**. Podocin Localizes in the Kidney to the Slit Diaphragm Area. *The American journal of pathology* 160: 131-139, 2002.
52. **Scimia MC, Hurtado C, Ray S, Metzler S, Wei K, Wang J, Woods CE, Purcell NH, Catalucci D, Akasaka T, Bueno OF, Vlasuk GP, Kaliman P, Bodmer R, Smith LH, Ashley E, Mercola M, Brown JH, and Ruiz-Lozano P**. APJ acts as a dual receptor in cardiac hypertrophy. *Nature* 488: 394-398, 2012.
53. **Shankland SJ, Pippin JW, Reiser J, and Mundel P**. Podocytes in culture: past, present, and future. *Kidney International* 72: 26-36, 2007.
54. **Sharma K, McCue P, and Dunn SR**. Diabetic kidney disease in the db/db mouse. *Am J Physiol Renal Physiol* 284: F1138-1144, 2003.
55. **Shin K, Kenward C, and Rainey JK**. Apelinergic System Structure and Function. *Comprehensive Physiology* 8: 407-450, 2017.
56. **Soler MJ, Wysocki J, and Batlle D**. ACE2 alterations in kidney disease. *Nephrol Dial Transplant* 28: 2687-2697, 2013.
57. **Soler MJ, Wysocki J, Ye M, Lloveras J, Kanwar Y, and Batlle D**. ACE2 inhibition worsens glomerular injury in association with increased ACE expression in streptozotocin-induced diabetic mice. *Kidney Int* 72: 614-623, 2007.
58. **Susztak K, Raff AC, Schiffer M, and Bottinger EP**. Glucose-induced reactive oxygen species cause apoptosis of podocytes and podocyte depletion at the onset of diabetic nephropathy. *Diabetes* 55: 225-233, 2006.
59. **Tamura J, Konno A, Hashimoto Y, and Kon Y**. Upregulation of renal renin-angiotensin system in mouse diabetic nephropathy. *Jpn J Vet Res* 2005;53(1–2):13–26.: 2005.
60. **Tang S-Y, Xie H, Yuan L-Q, Luo X-H, Huang J, Cui R-R, Zhou H-D, Wu X-P, and Liao E-Y**. Apelin stimulates proliferation and suppresses apoptosis of mouse osteoblastic cell line MC3T3-E1 via JNK and PI3-K/Akt signaling pathways. *Peptides* 28: 708-718, 2007.
61. **Tatemoto K, Hosoya M, Habata Y, Fujii R, Kakegawa T, Zou M-X, Kawamata Y, Fukusumi S, Hinuma S, Kitada C, Kurokawa T, Onda H, and Fujino M**. Isolation and Characterization of a Novel Endogenous Peptide Ligand for the Human APJ Receptor. *Biochemical and biophysical research communications* 251: 471-476, 1998.
62. **Thomas MC**. Pathogenesis and Progression of Proteinuria. *Diabetes and the Kidney Contrib Nephrol Basel, Karger*, vol 170: pp 48–56, 2011.
63. **Thomas PE, Wharram BL, Goyal M, Wiggins JE, Holzman LB, and Wiggins RC**. GLEPP1, a renal glomerular epithelial cell (podocyte) membrane protein-tyrosine phosphatase. Identification, molecular cloning, and characterization in rabbit. *Journal of Biological Chemistry* 269: 19953-19962, 1994.
64. **Umemoto S, Kuwabara T, Imamaki H, Hayata M, Izumi Y, Kakizoe Y, Mori K, and Mukoyama M**. [PS 01-26] THE ROLE OF ACTIVATED RENIN-ANGIOTENSIN SYSTEM FOR

THE MRP8/TLR4 SIGNALING IN DIABETIC NEPHROPATHY. *Journal of Hypertension* 34: e103, 2016.
65. **Vickers C, Hales P, Kaushik V, Dick L, Gavin J, Tang J, Godbout K, Parsons T, Baronas E, Hsieh F, Acton S, Patane M, Nichols A, and Tummino P**. Hydrolysis of biological peptides by human angiotensin-converting enzyme-related carboxypeptidase. *J Biol Chem* 277: 14838-14843, 2002.
66. **Wang L, de Kloet AD, Pati D, Hiller H, Smith JA, Pioquinto DJ, Ludin JA, Oh SP, Katovich MJ, Frazier CJ, Raizada MK, and Krause EG**. Increasing brain angiotensin converting enzyme 2 activity decreases anxiety-like behavior in male mice by activating central Mas receptors. *Neuropharmacology* 105: 114-123, 2016.
67. **Wang Z, Yu D, Wang M, Wang Q, Kouznetsova J, Yang R, Qian K, Wu W, Shuldiner A, Sztalryd C, Zou M, Zheng W, and Gong D-W**. Elabela-apelin receptor signaling pathway is functional in mammalian systems. *Scientific reports* 5: 8170-8170, 2015.
68. **Wolf G**. New insights into the pathophysiology of diabetic nephropathy: from haemodynamics to molecular pathology. *European Journal of Clinical Investigation* 34: 785-796, 2004.
69. **Wu H, Cheng XW, Hao C, Zhang Z, Yao H, Murohara T, and Dai Q**. Regulation of Apelin and Its Receptor Expression in Adipose Tissues of Obesity Rats with Hypertension and Cultured 3T3-L1 Adipocytes. *Experimental Animals* 63: 257-267, 2014.
70. **Wysocki J, Goodling A, Burgaya M, Whitlock K, Ruzinski J, Batlle D, and Afkarian M**. Urine RAS components in mice and people with type 1 diabetes and chronic kidney disease. *Am J Physiol Renal Physiol* ajprenal 00074 02017, 2017.
71. **Wysocki J, Ye M, Khattab AM, Fogo A, Martin A, David NV, Kanwar Y, Osborn M, and Batlle D**. Angiotensin-converting enzyme 2 amplification limited to the circulation does not protect mice from development of diabetic nephropathy. *Kidney Int* 91: 1336-1346, 2017.
72. **Xie H, Yuan L-Q, Luo X-H, Huang J, Cui R-R, Guo L-J, Zhou H-D, Wu X-P, and Liao E-Y**. Apelin suppresses apoptosis of human osteoblasts. *Apoptosis* 12: 247-254, 2007.
73. **Yamaleyeva LM, Chappell MC, Brosnihan KB, Anton L, Caudell DL, Shi S, McGee C, Pirro N, Gallagher PE, Taylor RN, Merrill DC, and Mertz HL**. Downregulation of apelin in the human placental chorionic villi from preeclamptic pregnancies. *American journal of physiology Endocrinology and metabolism* 309: E852-860, 2015.
74. **Yamaleyeva LM, Shaltout HA, and Varagic J**. Apelin-13 in blood pressure regulation and cardiovascular disease. *Current opinion in nephrology and hypertension* 25: 396-403, 2016.
75. **Yang P, Kuc RE, Brame AL, Dyson A, Singer M, Glen RC, Cheriyan J, Wilkinson IB, Davenport AP, and Maguire JJ**. [Pyr(1)]Apelin-13((1-12)) Is a Biologically Active ACE2 Metabolite of the Endogenous Cardiovascular Peptide [Pyr(1)]Apelin-13. *Front Neurosci* 11: 92-92, 2017.
76. **Yang P, Read C, Kuc RE, Buonincontri G, Southwood M, Torella R, Upton PD, Crosby A, Sawiak SJ, Carpenter TA, Glen RC, Morrell NW, Maguire JJ, and Davenport AP**. Elabela/Toddler Is an Endogenous Agonist of the Apelin APJ Receptor in the Adult Cardiovascular System, and Exogenous Administration of the Peptide Compensates for the Downregulation of Its Expression in Pulmonary Arterial Hypertension. *Circulation* 135: 1160-1173, 2017.
77. **Ye M, Wysocki J, William J, Soler MJ, Cokic I, and Batlle D**. Glomerular localization and expression of Angiotensin-converting enzyme 2 and Angiotensin-converting enzyme: implications for albuminuria in diabetes. *J Am Soc Nephrol* 17: 3067-3075, 2006.
78. **Zeng H, He X, Hou X, Li L, and Chen J-X**. Apelin gene therapy increases myocardial vascular density and ameliorates diabetic cardiomyopathy via upregulation of sirtuin 3. *American Journal of Physiology-Heart and Circulatory Physiology* 306: H585-H597, 2014.

79. **Zhang H, Gong D, Ni L, Shi L, Xu W, Shi M, Chen J, Ai Y, and Zhang X**. Serum Elabela/Toddler Levels Are Associated with Albuminuria in Patients with Type 2 Diabetes. *Cellular Physiology and Biochemistry* 48: 1347-1354, 2018.
80. **Zhang S-Y, Marlier A, Gribouval O, Gilbert T, Heidet L, Antignac C, and Gubler MC**. In vivo expression of podocyte slit diaphragm-associated proteins in nephrotic patients with NPHS2 mutation. *Kidney International* 66: 945-954, 2004.
81. **Zhang Z, Yu B, and Tao G-z**. Apelin protects against cardiomyocyte apoptosis induced by glucose deprivation. *Chin Med J (Engl)* 122: 2360-2365, 2009.
82. **Zhe C, Di W, Lanfang L, and Linxi C**. Apelin/APJ System: A Novel Therapeutic Target for Myocardial Ischemia/Reperfusion Injury. *DNA and Cell Biology* 35: 766-775, 2016.
83. **Zhong J-C, Yu X-Y, Huang Y, Yung L-M, Lau C-W, and Lin S-G**. Apelin modulates aortic vascular tone via endothelial nitric oxide synthase phosphorylation pathway in diabetic mice. *Cardiovascular Research* 74: 388-395, 2007.

Eidesstattliche Versicherung

Ich, Tilman Müller, versichere an Eides statt durch meine eigenhändige Unterschrift, dass ich die vorgelegte Dissertation mit dem Thema: „Apelinergic system in the kidney: implications for diabetic kidney disease“ selbstständig und ohne nicht offengelegte Hilfe Dritter verfasst und keine anderen als die angegebenen Quellen und Hilfsmittel genutzt habe.

Alle Stellen, die wörtlich oder dem Sinne nach auf Publikationen oder Vorträgen anderer Autoren beruhen, sind als solche in korrekter Zitierung kenntlich gemacht. Die Abschnitte zu Methodik (insbesondere praktische Arbeiten, Laborbestimmungen, statistische Aufarbeitung) und Resultaten (insbesondere Abbildungen, Graphiken und Tabellen) werden von mir verantwortet.

Meine Anteile an etwaigen Publikationen zu dieser Dissertation entsprechen denen, die in der untenstehenden gemeinsamen Erklärung mit dem/der Betreuer/in, angegeben sind. Für sämtliche im Rahmen der Dissertation entstandenen Publikationen wurden die Richtlinien des ICMJE (International Committee of Medical Journal Editors; www.icmje.og) zur Autorenschaft eingehalten.

Ich erkläre ferner, dass mir die Satzung der Charité – Universitätsmedizin Berlin zur Sicherung Guter Wissenschaftlicher Praxis bekannt ist und ich mich zur Einhaltung dieser Satzung verpflichte.

Die Bedeutung dieser eidesstattlichen Versicherung und die strafrechtlichen Folgen einer unwahren eidesstattlichen Versicherung (§§156, 161 des Strafgesetzbuches) sind mir bekannt und bewusst.

Datum Unterschrift

Anteilserklärung an erfolgten Publikationen

Tilman Müller hatte folgenden Anteil an den folgenden Publikationen:

Publikation 1:

Tilman Müller, Anastasia Z. Kalea, Alonso Marquez, Ivy Hsieh, Syed Haque, Minghao Ye, Jan Wysocki, Michael Bader, Daniel Batlle
Apelinergic system in the kidney: implications for diabetic kidney disease, Physiological Reports, 12/2018, 6(23), e13939, doi: 10.14814/phy2.13939

Beitrag im Einzelnen: Die Publikation wurde größtenteils durch mich in Zusammenarbeit mit Professor Batlle verfasst. Weiterhin gehen auf mich die Auswertung des Caspase-3 Assays und der Immunhistologie zurück. Daraus sind in Zusammenarbeit mit Minghao Ye und Jan Wysocki die Abbildungen 2-5 sowie 9c entstanden. Figur 7 entstand aus meiner statistischen Auswertung. Die Abbildung 9c ist ein Beispiel eines Immunhistochemievergleichs zwischen *db/m* und *db/db* Mäusen, bei dem ich als einer der verblindenen Kontrolleure agierte. Außerdem führte ich die RT-PCR Experimente der kultivierten Zellkulturen (Abschnitt: „Effect of high glucose environment and Ang II on APJ and preproapelin mRNA expression“) sowie der Telmisartan-Studie durch (Abschnitt: „Effect of Telmisartan on APJ in *db/db* kidney“). Daraus resultierten die Abbildungen 8 und 10.

_____

Unterschrift, Datum und Stempel des betreuenden Hochschullehrers

_____

Unterschrift des Doktoranden

Mein Lebenslauf wird aus datenschutzrechtlichen Gründen in der elektronischen Version meiner Arbeit nicht veröffentlicht.

Publikationsliste

Publikationen:

Tilman Müller, Anastasia Z. Kalea, Alonso Marquez, Ivy Hsieh, Syed Haque, Minghao Ye, Jan Wysocki, Michael Bader, Daniel Batlle
Apelinergic system in the kidney: implications for diabetic kidney disease, Physiological Reports, 12/2018, 6(23), e13939, doi: 10.14814/phy2.13939

Posterpräsentationen:

Tilman Müller, Pan Liu, Jan Wysocki, Peter Serfozo, Minghao Ye, Jing Jin, Daniel Batlle
Evaluation of efficiencies for carboxy-terminal phenylalanine cleavage from Angiotensin II and III and Apelin peptides by Angiotensin-Converting-Enzyme 2 using a new fluorimetric method
American Heart Association, San Francisco, USA 09/2017

Jan Wysocki, **Tilman Müller**, Pan Liu, Jing Jin, Daniel Batlle
A novel approach for evaluation of cleavage of angiotensin peptides by their angiotensinase partners.
American Society of Nephrology, New Orleans, USA 10/2017

Danksagung

An dieser Stelle möchte ich mich zuerst bei Prof. Dr. Michael Bader für die Möglichkeit bedanken, meine Doktorarbeit unter seiner Betreuung anfertigen zu können. Sehr schnell lernte ich seine ruhige, analytische Art zu schätzen sowie sein aufrichtiges Interesse daran, dieser Arbeit zu einem Erfolg zu verhelfen. Dies war mir in schwierigen Zeiten oft eine wichtige Stütze.

Weiterhin gebührt mein aufrichtiger Dank Prof. Dr. Daniel Batlle sowie seinen Mitarbeitern Dr. Jan Wysocki und Dr. Minghao Ye für die Möglichkeit in ihrem Labor zu arbeiten und ohne die folglich das Abenteuer Amerika nicht möglich gewesen wäre. Ich profitierte sehr von Prof. Batlles Expertise in der Forschung und seinen Ideen für weiterführende Experimente, die den Arbeitsfluss am Laufen hielten, und seiner freundlichen Art inner- und außerhalb des Labors. Dr. Jan Wysocki möchte ich ebenfalls besonders hervorheben, da er mich stets bei meinen Experimenten unterstützte und immer eine helfende Hand oder auch ein zuhörendes Ohr für mich hatte. Bei ihm wie auch bei Prof. Bader hatte ich jederzeit das Gefühl für jedes Problem eine Lösung zu finden.
Bei Dr. Minghao „Golden Hands“ Ye möchte ich mich für die zuverlässige Ausführung und Hilfe bei wichtigen Experimenten, insbesondere der Immunhistologie, bedanken.
Meiner Laborpartnerin Jeannette Tang möchte ich für die gemeinsame Zeit (beginnend mit dem Chicago Hand Shake) und die zahlreichen gemeinsamen Mittags- und Kaffeepausen danken und zeitgleich beglückwünsche ich sie zu ihrer erfolgreichen Publikation.

Ebenfalls möchte ich an dieser Stelle meine Mitbewohner Carlos Gallo, Julia Dawson und William Steinfeld sowie meinen Kletter-Partner Reinier hervorheben. Ohne sie wäre meine Zeit nicht halb so ereignisreich gewesen und über die Monate sind sie mir sehr gute Freunde geworden. Ich hoffe, den ein oder anderen auch mal in Deutschland begrüßen zu können!

In diesem Sinne möchte ich mich bei all meinen Freunden für die Gespräche und insbesondere bei Johanna Angermaier, Aileen Braun, Anne Nasert und Matthias Ortloff für ihre Besuche herzlich bedanken. Sie waren mir eine willkommene und oft sehr nötige Abwechslung zum Arbeitsalltag und waren mir immer eine Brücke in die Heimat.

Ich danke dem Biomedical Education Program (BMEP) für die finanzielle Unterstützung und die Zusammenführung mit anderen jungen, enthusiastischen Forschern für den Austausch von Tipps und Erfahrungen zum Leben und Forschen im Ausland.

Bei Anna Löwa möchte ich mich für das professionelle Shooting bedanken und empfehle sie auch gerne an kommende Doktoranden weiter, die noch auf der Suche nach dem perfekten Bild von sich sind.

Zu guter Letzt gilt mein herzlichster Dank meiner Familie um meine Mutter Katrin, meinen Vater Volkmar und meinen Bruder Gerrit sowie meinen Großeltern, deren andauernder Unterstützung ich mir jederzeit bewusst war und die mich schlussendlich auch dazu gebracht hat, neue Wege zu wagen.